

Final Report, Addendum

February 1972

Development of a Simulation Program for a Full Size Remote Manipulator System

Preliminary Design of a Shuttle Docking and Cargo Handling System

| | |
|---|--|
| (NASA-CR-141567) DEVELOPMENT OF A SIMULATION PROGRAM FOR A FULL SIZE REMOTE MANIPULATOR SYSTEM. PRELIMINARY DESIGN OF A SHUTTLE DOCKING AND CARGO HANDLING SYSTEM, ADDENDUM Final Report (Martin-Marietta | N77-77598 Unclas 00/18 28839 |
|---|--|

REPRODUCED BY
**NATIONAL TECHNICAL
 INFORMATION SERVICE**
 U S DEPARTMENT OF COMMERCE
 SPRINGFIELD, VA. 22161

MARTIN MARIETTA DENVER
 DIVISION


DEVELOPMENT OF A
SIMULATION PROGRAM FOR
A FULL SIZE REMOTE
MANIPULATOR SYSTEM

PRELIMINARY DESIGN OF
A SHUTTLE DOCKING AND
CARGO HANDLING SYSTEM

Prepared by

W. Burkitt
F. Greeb
A. Ray
A. Wudell
J. Yatteau

Approved



Shepard B. Brodie
Program Manager

MARTIN MARIETTA CORPORATION
P.O. Box 179
Denver, Colorado 80201

FOREWORD

The results of work performed by Martin Marietta Corporation's Denver Division while under contract to NASA Manned Spacecraft Center are documented in this report entitled *Development of a Simulation Program for a Full Size Remote Manipulator System*. This report is submitted in fulfillment of an addition to Contract NAS9-11932 covering *Preliminary Design of a Shuttle Docking and Cargo Handling System*. The NASA Technical Monitor for the Contract was Mr. Richard B. Davidson, of the Spacecraft Design Division, engineering Technology Branch.

CONTENTS

| | <u>Page</u> |
|--|------------------------|
| Foreword | iii |
| I. Introduction | I-1 |
| II. RMS Mission Requirements | II-1 |
| A. Functional Breakdown of RMS Missions | II-1 |
| B. Dynamic State | II-7 |
| C. Work Envelope | II-14 thru II-16 |
| III. Critical Simulation Requirements | III-1 |
| A. Degrees of Freedom Required | III-1 |
| B. Orientation of Task in Simulator | III-4 thru III-6 |
| IV. Simulation Methods | IV-1 |
| A. Airpad (Six Degrees of Freedom) | IV-4 |
| B. Cable Suspension | IV-8 |
| C. Servo-Driven | IV-12 |
| D. Neutral Buoyancy | IV-15 thru IV-21 |
| V. Comparison of Simulation Methods | V-1 |
| A. Factors of Comparison | V-1 |
| B. Conclusions of Comparison | V-5 thru V-7 |
| VI. Manipulator Structural Design Alternatives | VI-1 |
| A. Zero-G Design | VI-1 |
| B. Structural Design for One-Inch Deflection | VI-5 |
| C. Twelve-Inch Diameter Arm Sections | VI-8 |
| D. External Stiffening Technique | VI-10 thru VI-12 |

Preceding page blank

| | | |
|-------|--|--------------------------|
| VII. | Investigation of Options for Selected Simulation Method (Airpad) | VII-1 |
| | A. Airpad - Five Degrees of Freedom | VII-1 |
| | B. Airpad - Five Degrees and Counterbalance - One Degree | VII-3 thru VII-5 |
| VIII. | Mission Simulation Capability of Airpad Simulator | VIII-1 |
| | A. Simulator Capability by Mission Element | VIII-1 |
| | B. Summary | VIII-3 thru VIII-4 |

Appendixes

| | | |
|---|---|---------------------|
| A | Dynamical Analysis | A-1 thru A-12 |
| B | Optional Rotation of RMS Operator's Field of View | B-1 thru B-5 |
| C | Center of Gravity Location for Six-Degree-of-Freedom Airpad Simulator | C-1 thru C-3 |
| D | Dynamical Aspects of Airpad Simulations | D-1 thru D-9 |
| E | Statement of Work, Task Identification | E-1 |

Figure

| | | |
|-------|--|-------|
| II-1 | Space Station Module Unload, Transfer and Dock | II-3 |
| II-2 | Payload Deployment | II-5 |
| II-3 | RMS Plane-of-Action | II-15 |
| III-1 | Dynamic Model for Mission Elements | III-1 |
| IV-1 | Airpad -- Six Degrees of Freedom | IV-5 |
| IV-2 | Cable Suspension | IV-10 |

| | | |
|--------------|---|--------|
| IV-3 | Simulation Flow Chart | IV-13 |
| IV-4 | Servo-Driven | IV-14 |
| IV-5 | Neutral Buoyancy Facility for Complete RMS Work Envelope | IV-16 |
| IV-6 | Adaptation of MSFC Facility for RMS Simulation | IV-17 |
| IV-7 | Optimal Use of MSFC Facility for RMS Simulation | IV-18 |
| VI-1 | Loading Conditions Due to Design Loads | VI-2 |
| VI-2 | Loading Conditions Due to Structure Weight | VI-4 |
| VII-1 | Airpad - Five Degrees of Freedom | VII-2 |
| VII-2 | Airpad - Five Degrees and Counterbalance - One Degree | VII-4 |
| <u>Table</u> | | |
| II-1 | LST Servicing | II-8 |
| II-2 | Dynamic State by Mission Element | II-13 |
| IV-1 | Comparison of Servo-Driven and Natural Reaction Simulation Modes | IV-3 |
| V-1 | Simulation Method Dynamic State Capability | V-2 |
| V-2 | Simulation of Comparison Factors | V-6 |
| VIII-1 | Airpad Simulator Capability by Simulator Element | VIII-4 |

I. INTRODUCTION

The objective of this study is to investigate alternative simulation methods that could be used to simulate zero-g operation of a Remote Manipulator System (RMS). Man-in-the-loop simulator methods considered were restricted to those in which a full size manipulator arm could be incorporated. Other types of simulators that could be used for various subsystem level design tradeoffs were not included. Emphasis was placed on desirability to incorporate in the simulation real mass and inertia properties.

This final report describes work conducted during the study program. Chapter II covers the requirements for RMS space missions in terms of RMS functions, dynamic states, and work envelopes. The critical simulation requirements presented in Chapter III include degrees of freedom and orientation of task with respect to gravity. In Chapter IV airpad, cable suspension, servo-driven, and neutral buoyancy simulation methods are described and design considerations presented. A comparison of these simulation methods is contained in Chapter V. The final three chapters describe the study effort that was expended after the most effective simulation method was selected. Chapter VI discusses design aspects of a full size remote manipulator arm that will operate in one-g environment. Chapters VII and VIII cover airpad simulator options and mission simulation capabilities.

II. RMS MISSION REQUIREMENTS

Requirements of space mission elements covered in this chapter constitute a detailed definition for simulation considerations of the space problem. Simulations used to investigate RMS performance ideally should duplicate these requires as closely as possible.

The space mission elements studied include:

- 1) Unstowage and deployment of RMS;
- 2) Berthing Shuttle to Space Station or other orbital payloads;
- 3) Cargo transfer;
- 4) Deployment of payloads;
- 5) Retrieval of orbiting payloads;
- 6) Maintenance on orbiting vehicles and payloads--Shuttle docked;
- 7) Maintenance on orbiting vehicles and payloads--Shuttle not docked.

For each mission element, the RMS functions, dynamic state, and work envelope are defined.

A. FUNCTIONAL BREAKDOWN OF RMS MISSIONS

This subsection describes the RMS functional requirements, according to the various elements of a Shuttle mission, which require RMS operation. These mission elements are described according to the tasks of which they are comprised.

1. Unstowage and Deployment of RMS (Mission Element No. 1)

This mission element is prerequisite to any other RMS mission element and is comprised of the following tasks:

- a) Unstow RMS (including manipulators and associated equipment);

- b) Deploy manipulator(s);
- c) Maneuver manipulator to standby position or position for next mission element.

2. Berthing Shuttle-to-Space-Station or Other Payloads (Mission Element No. 2)

Two alternatives for the function of the RMS during this mission element are being considered: (1) the manipulator is envisioned as being used strictly as a sensor of the close-in relative position between the Shuttle and the docking target; (2) the manipulator exercises its torque capability to assist in eliminating the relative motion of the two bodies.* For purposes of this report the first alternative is chosen and therefore it is assumed that energy for the maneuver will be supplied by the Shuttle thrusters. Further, it is assumed that the initial relative motion of the two bodies is such that the manipulator can attach to and move with the target in such a way that only small forces of interaction are generated.

This mission element is comprised of the following tasks:

- a) Maneuver manipulator to target attachment interface;
- b) Attach terminal device to target attachment interface;
- c) Set manipulator actuator systems to docking mode;
- d) Provide positional and velocity information to the Shuttle control system;
- e) Release terminal device from target attachment interface;
- f) Maneuver manipulator to standby position or position for next element.

3. Cargo Transfer (Mission Element No. 3)

The mission element consists of transferring and docking Space Station modules from the cargo bay of the Shuttle to the Space Station. (See Fig. II-1.)

During this mission element the Shuttle will be docked to the Space Station. The Remote Manipulator System (RMS) will be transferring mass from one point to another in the combined Shuttle/Space Station. The combined system will be drifting with residual angular and linear velocities.

*A third alternative is a combination of these two.

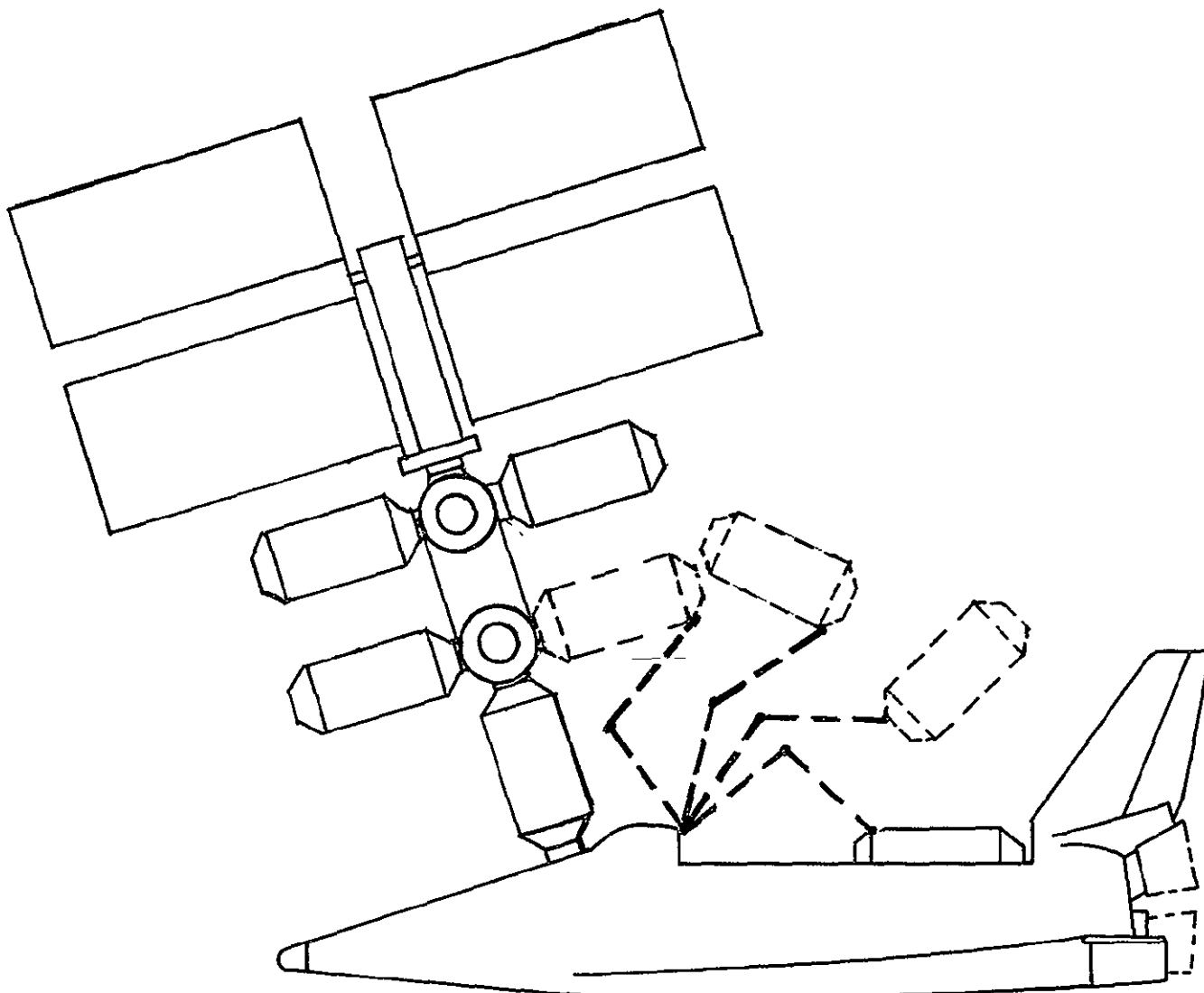


Fig. II-1' Space Station Module Unload, Transfer and Dock

The mission element is comprised of the following tasks:

- a) Maneuver manipulator to cargo attachment interface;
- b) Attach manipulator to cargo with terminal device;
- c) Unstow and remove cargo from cargo bay;
- d) Transfer cargo to docking area on Space Station;
- e) Dock cargo to Space Station docking port;
- f) Release terminal device from cargo attachment interface;
- g) Maneuver manipulator to standby position or position for next mission element.

4. Deployment of Payloads (Mission Element No. 4)

In this mission element, the payload is removed from the cargo bay and deployed using the extended manipulator. (See Fig. II-2.) It is assumed that the Shuttle is oriented properly before the manipulator is extended. Then the payload can be deployed as soon as the manipulator has been extended to its end position.

The mission element is comprised of the following tasks:

- a) Maneuver manipulator to payload (cargo) attachment interface;
- b) Attach terminal device to payload;
- c) Unstow and remove payload from cargo bay;
- d) Transfer payload to deployment point;
- e) Deploy payload;
- f) Maneuver manipulator to standby position or position for next mission element.

5. Retrieval of Orbiting Payloads (Mission Element No. 5)

For this mission element, the Shuttle will fly to a station-keeping point relative to the payload to be retrieved. The relative angular and linear velocities will be arrested as accurately as possible, and then the thrusters will not be fired again during the retrieval. This will result in some residual relative angular and linear velocities.

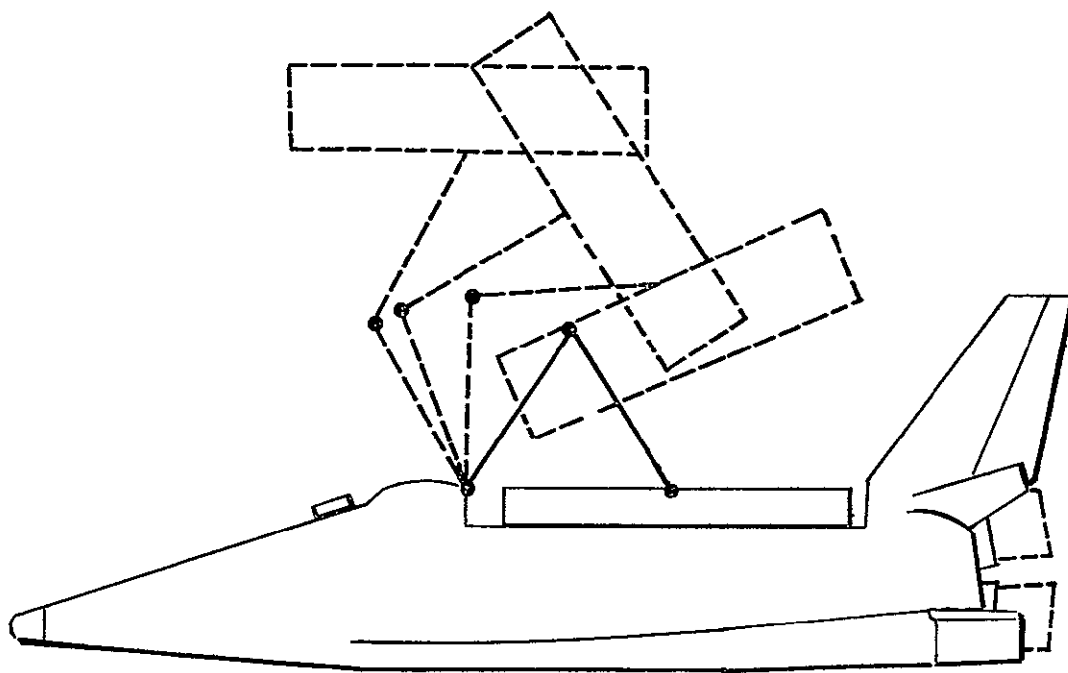


Fig. II-2 Payload Deployment

The payloads may include some that are slowly tumbling or spinning. The tumble or spin will be slow enough that spinup of the manipulator terminal device will not be required.

Grappling will be performed with the manipulator terminal device.

The mission element is comprised of the following tasks:

- a) Maneuver manipulator to region of target;
- b) Maneuver terminal device to attach/grapple target;
- c) Maneuver manipulator with attached target to Shuttle cargo bay;
- d) Dock cargo to Shuttle pallet in cargo bay;
- e) Release terminal device from cargo attachment interface;
- f) Maneuver manipulator to standby position or position for next mission element.

6. Maintenance on Orbiting Vehicles and Payloads - Shuttle Docked (Mission Element No. 6)

For this mission element, the Shuttle is docked with the orbiting vehicle or payload. Servicing and maintenance includes replacement of modules. If tasks requiring a high degree of dexterity are to be run, this capability will have to be incorporated in the terminal device.

The mission element is comprised of the following tasks:

- a) Maneuver manipulator to region of maintenance module on vehicle to be serviced;
- b) Attach terminal device to module;
- c) Remove module from vehicle;
- d) Transfer module to cargo bay;
- e) Stow module in cargo bay;
- f) Maneuver manipulator to region of replacement module in cargo bay;
- g) Attach terminal device to module;
- h) Unstow and remove module from cargo bay;
- i) Transfer module to maintenance region on vehicle;

- j) Replace module on vehicle;
- k) Release terminal device from maintenance module attachment interface;
- l) Maneuver manipulator to standby position or position for next mission element.

7. Maintenance on Orbiting Vehicles and Payloads-Shuttle Not Docked (Mission Element No. 7)

This mission element is the same as mission element No. 6 except the Shuttle is not docked to the payload. The subtasks to be performed are the same. The interactions between the manipulator and the payload will be different.

8. Large Space Telescope Servicing

The previously described mission elements were used in the study to determine simulation requirements and design considerations. Goodard Space Flight Center provided Table II-1, which is included in this report as a more specific example of these mission elements.

B. DYNAMIC STATE

The RMS tasks listed in the previous section were analyzed for the first seven mission elements to determine the character of the forces and motions involved. All foreseeable contributions to the dynamic state, regardless of their magnitudes, were included. Motions and forces that were similar in character although of varying magnitudes were treated the same. For example, motions and forces during cargo transfer were considered as equivalent although they differ in magnitude if the Shuttle is berthed or if it is unberthed (due to the increased system mass).

1. Dynamic State by Task

a. Unstowage and Deployment of RMS (Mission Element No. 1)

Task a Unstow RMS.- Unstowing the RMS will not influence the dynamic state of the system.

Table II-1 LST Servicing*

| PAYLOAD FREE IN SPACE ¹ | FUNCTION | NEEDS SIMULATION | MOTION ² |
|------------------------------------|---|------------------|---------------------|
| | <u>Erection</u> | | |
| No | a Disengagement (of a holding clamp) | Yes | ⊥ To plane |
| Yes | b. Elevation (unload) | Yes | Plane |
| Yes | c Deployment of appendage | Yes | Plane |
| Yes | d Release | Yes | Plane |
| Yes | e Checkout (spacecraft preferred orientation) | Yes | Plane |
| Yes | f Umbilicals (plugging and unplugging) | Yes | ⊥ To plane |
| | <u>Docking (manipulator to LST)</u> | | |
| Yes | a. Approach Spacecraft with Shuttle | No | |
| Yes | b Closing with manipulator | Yes | Plane |
| Yes | c. Capture latching | Yes | Plane |
| Yes | d Holding | No | |
| Yes | e. Umbilicals (plugging and unplugging) | Yes | ⊥ To plane |
| | <u>Retrieval</u> | | |
| Yes | a. Rotation | Yes | Plane |
| Yes | b. Retraction into cargo bay | Yes | Plane |
| Yes | c. LST placement into trunion ring | Yes | Plane |
| No | d Locking LST | Yes | ⊥ To plane |
| No | e. Umbilicals (plugging and unplugging) | Yes | ⊥ To plane |
| | <u>Resupply (assuming manipulator)</u> | | |
| | a. Repeat docking functions a-e | | |
| Yes | b. Latching of module from LST | Yes | Plane |
| Yes | c. Removal of module from LST | Yes | Plane |
| Yes | d Storing module in bay | Yes | Plane |
| No | e Grabbing new module in bay | Yes | plane |
| Yes | f. Inserting new module on LST | Yes | Plane |
| Yes | g Release LST | Yes | Plane |
| | <u>Resupply (assuming exchanger platform mounted in bay)</u> | | |
| | a Repeat docking functions a-e | | |
| Yes | b Bring LST down in preferred orientation | Yes | Plane |
| No | c Latch LST to platform in Shuttle bay | Yes | ⊥ To plane |
| | d Repeat a to c in reverse | | |
| | <u>Resupply (assuming exchanger elevated above bay via manipulator arm)</u> | | |
| | a. Repeat docking functions | | |
| Yes | b. Bring platform from out of bay with other arm to under side of LST | | |
| No | c Latch platform to LST | Yes | Plane |
| No | d Hold with arm | No | Plane |
| No | e Release arm | Yes | Plane |
| | f Reverse steps a to c above | | |

*An example provided by Goddard SFC

1. Differentiates whether the payload is in space or in cargo bay.
2. The primary intended motion is either in X-Z plane or perpendicular (⊥) to it.

- Task b Deploy manipulator(s).
Forces: Joint torques will be required to deploy the manipulator and, therefore, reactions to these torques will act on the Shuttle.
Motion: The manipulator motion relative to the Shuttle can be expected to involve all of the joint degrees of freedom (DOF). The Shuttle will be moving with six DOF in inertial space. The reaction torques due to manipulator deployment will induce a slight perturbation in this motion.
- Task c- Maneuver manipulator to standby position or position for next mission element.- The forces and motions have the same character as in task 1.b.

b. Berthing Shuttle-to-Space-Station or Other Payloads
(Mission Element No. 2)

- Task a Maneuver manipulator to target attachment interface. - The forces and motions have the same character as in task 1.b.
- Task b Attach terminal device to target attachment interface. -
Forces: There will be impact forces between the terminal device and attachment interface. These forces will be transmitted through the manipulator to the Shuttle.
Motion: The motion of the manipulator relative to the Shuttle will be minimal during this task. The motion of the Shuttle relative to the Space Station will be perturbed slightly by the impact forces. The motion of the Space Station in inertial space will also be perturbed slightly.
- Task c Set manipulator actuator systems/to docking mode.- This task will not affect the dynamic state of the system.
- Task d Provide position and force information to the Shuttle control system.-
Forces: Due to friction at the joints, there will be torques acting on the arms; hence, there will be reaction torques acting on the Shuttle will Space Station.

Motion: The motion of the manipulator relative to the Shuttle will involve, to some degree, all joint DOF.

The motion of the Shuttle relative to the Space Station will entail six DOF.

The motion of the Space Station in inertial space will also involve six DOF.

Tasks e and f Release terminal device from target docking attachment interface and maneuver manipulator to standby position. - The motion and forces have the same character as in task 1.b.

c. Cargo Transfer (Mission Element No. 3)

Task a Maneuver manipulator to cargo attachment interface.- The characteristics of the motion and forces are the same as task 1.b.

Task b Attach manipulator to cargo with terminal device. -
Forces: There will be impact forces between the terminal device and the cargo.
Motion: The motion of the manipulator relative to the Shuttle will be minimal during this task. The impact forces will have o effect on the motion of the Shuttle/Space Station combination.

Task c and d Unstow, remove and transfer cargo to docking on Space Station -
Forces: Larger joint torques will be required to move the cargo/manipulator combination; hence, larger reaction torques will be acting on the Shuttle/Space Station combination.
Motion: The motion will have the same characteristics as in task 1.b.

Task e Dock cargo to Space Station docking port. - The motion and forces have the same character as in task 3.b. The impact forces will have greater magnitudes.

Tasks f and g Release cargo and maneuver manipulator to standby position.- The motion and forces have the same character as in task 1.b.

d. Deployment of Payloads (Mission Element No. 4)

Task a Maneuver manipulator to payload attachment interface.- The forces and motion have the same characteristics as in task 3.b.

Task b Attach terminal device to payload. - The forces and motion have the same characteristics as in task 3.b.

Task c Unstow and remove payload from cargo bay. - The forces and motion have the same characteristics as in task 3.c.

Task d Transfer payload to deployment point. - The forces and motion have the same characteristics as in task 3.d.

Task e Deploy payload.- Forces and motion: The deployment of the payload will produce a reaction force on the Shuttle which, in turn, will perturb the motion of the Shuttle in inertial space. The size of the perturbation will depend on the mass of payload and velocity of deployment.

Task f Maneuver manipulator to standby position.- The forces and motion have the same characteristics as in task 1.b.

e. Retrieval of Orbiting Payloads (Mission Element No. 5)

Task a Maneuver manipulator to region of target - The forces and motion have the same characteristics as in task 1.b.

Task b Maneuver terminal device to attach/grapple target.- Forces: There will be contact forces between the manipulator and corresponding reaction forces on the Shuttle. The magnitude of these forces will depend on the inertia properties of the target and Shuttle prior to attachment.

Motion: The motion of the manipulators relative to the Shuttle will be minimal during this subtask. Prior to attachment, the target will be moving with six DOF relative to the Shuttle and during this subtask, this motion will be arrested. The Shuttle will be moving with six DOF in inertial space and this motion will be perturbed by the reaction forces developed by grappling with the target.

Task c through f Maneuver to cargo bay, dock cargo to bay pallet, release cargo and maneuver to standby position.- Motions and forces have the same characteristics as tasks 3.d. through 3.g.

f. Maintenance on Orbiting Vehicles and Payloads - Shuttle Docked (Mission Element No. 6)

For this mission element, the Shuttle is docked with the orbiting vehicle or payload. Servicing and maintenance includes replacement of modules. If tasks requiring a high degree of dexterity are to be run, this capability will have to be incorporated in the terminal device.

The motion and forces occurring in these tasks have the same characteristics as in the cargo transfer tasks.

g. Maintenance on Orbiting Vehicles and Payloads - Shuttle Not Docked (Mission Element No. 7)

This mission element is the same as No. 6 except the Shuttle is not docked to the payload. The series of tasks to be performed are the same. The interactions between the manipulator and the payload will be different.

The motion and forces arising from this mission element have the same characteristics as the retrieval of orbiting payloads.

2. Dynamic State by Mission Element

A summary of the forces and motions associated with each mission element is given in Table II-2. The dynamical features that are listed include any motion or forces that occur at any time during a particular mission and not just those which are present

Table II-2 Dynamic State by Mission Element

| DYNAMICAL FEATURES | | MISSION ELEMENT | | | | | | |
|--------------------|---|---|---|--|---|---|---|---|
| | | 1) UNSTOWAGE AND DEPLOYMENT | 2) BERTHING SHUTTLE | 3) CARGO TRANSFER | 4) DEPLOYMENT OF PAYLOADS | 5) RETRIEVAL | 6) MAINTENANCE (SHUTTLE DOCKED) | 7) MAINTENANCE (SHUTTLE NOT DOCKED) |
| FORCES AND TORQUES | Shuttle | Reaction to joint torques | Reaction to joint torques and impact forces between manipulator and Space Station | Reaction to joint torques and impact forces between manipulator and cargo | Same character as mission element No. 3 | Same character as mission element No. 3 | Same character as mission element No. 3 | Same character as mission element No. 3 |
| | Manipulator | Joint torques | Joint torques and impact forces from contact with Space Station | Joint torques and impact forces between manipulator and cargo | Same character as mission element No. 3 | Same character as mission element No. 3 | Same character as mission element No. 3 | Same character as mission element No. 3 |
| | Space Station or other orbiting vehicle | Not involved | Impact forces and reactions to friction torques at joints | Space Station is docked to Shuttle and therefore experiences same forces and torques | Not involved | Not involved | Same character as mission element No. 3 | Contact forces from manipulator |
| | Cargo or payload | Not involved | Not involved | contact forces from manipulator | Same character as mission element No. 3 | Same character as mission element No. 3 | Same character as mission element No. 3 | Same character as mission element No. 3 |
| MOTION | Shuttle | 3 rotational and 3 translational DOF relative to inertial space | Same character as mission element No. 1 | Same character as mission element No. 1 | Same character as mission element No. 1 | Same character as mission element No. 1 | Same character as mission element No. 1 | Same character as mission element No. 1 |
| | Manipulator | Motions involving all joint DOF | Same character as mission element No. 1 | Same character as mission element No. 1 | Same character as mission element No. 1 | Same character as mission element No. 1 | Same character as mission element No. 1 | Same character as mission element No. 1 |
| | Space Station or other orbiting vehicle | Not involved | 3 rotational and 3 translational DOF relative to Shuttle | Same motion as Shuttle | Not involved | Not involved | Same character as mission element No. 3 | Same character as mission element No. 2 |
| | Cargo or payload | Not involved | Not involved | 3 rotational and 3 translational DOF relative to Shuttle | Same character as mission element No. 3 | Same character as mission element No. 3 | Same character as mission element No. 3 | Same character as mission element No. 3 |

continuously. Further, only the characteristics of the dynamical features are described, with no attempt being made to differentiate between mission elements with respect to the magnitudes of the various features.

It is recalled that all foreseeable dynamic effects that will occur during space operation have been included in the foregoing description. A discussion pertaining to which of these effects is essential to a ground simulation is presented in Chapter 3, Section A.

C. WORK ENVELOPE

When defining the RMS work envelope in preparation for investigating simulation methods, it is important that one general simulator characteristic be considered, namely, that most simulators can be designed to provide large travel nominally in a plane much more readily than in all degrees of freedom. Frequently the validity of the nominally planar simulator is better, and at the same time the simulator fabrication cost is lower.

The RMS reach envelope bounds all possibilities of the RMS work envelope relative to the Shuttle. Certainly, the work envelope must fall within these bounds. There are three specific points of interest relative to the manipulator arm positions while performing the cargo transfer tasks. These points, noted in Fig. II-3 are:

- a) Operator's viewing point;
- b) Terminal device attachment point when the target is in the initial position;
- c) Terminal device attachment point when the target is in the end position.

These three points define a plane that can be thought of as the RMS task plane-of-action. The task, as the pilot will see it, is to move the cargo from B to C in a straight line within the controllability of the RMS. Therefore, the RMS terminal device will nominally be confined to a plane-of-action. However, the manipulator elbow will not necessarily be confined to the plane-of-action.

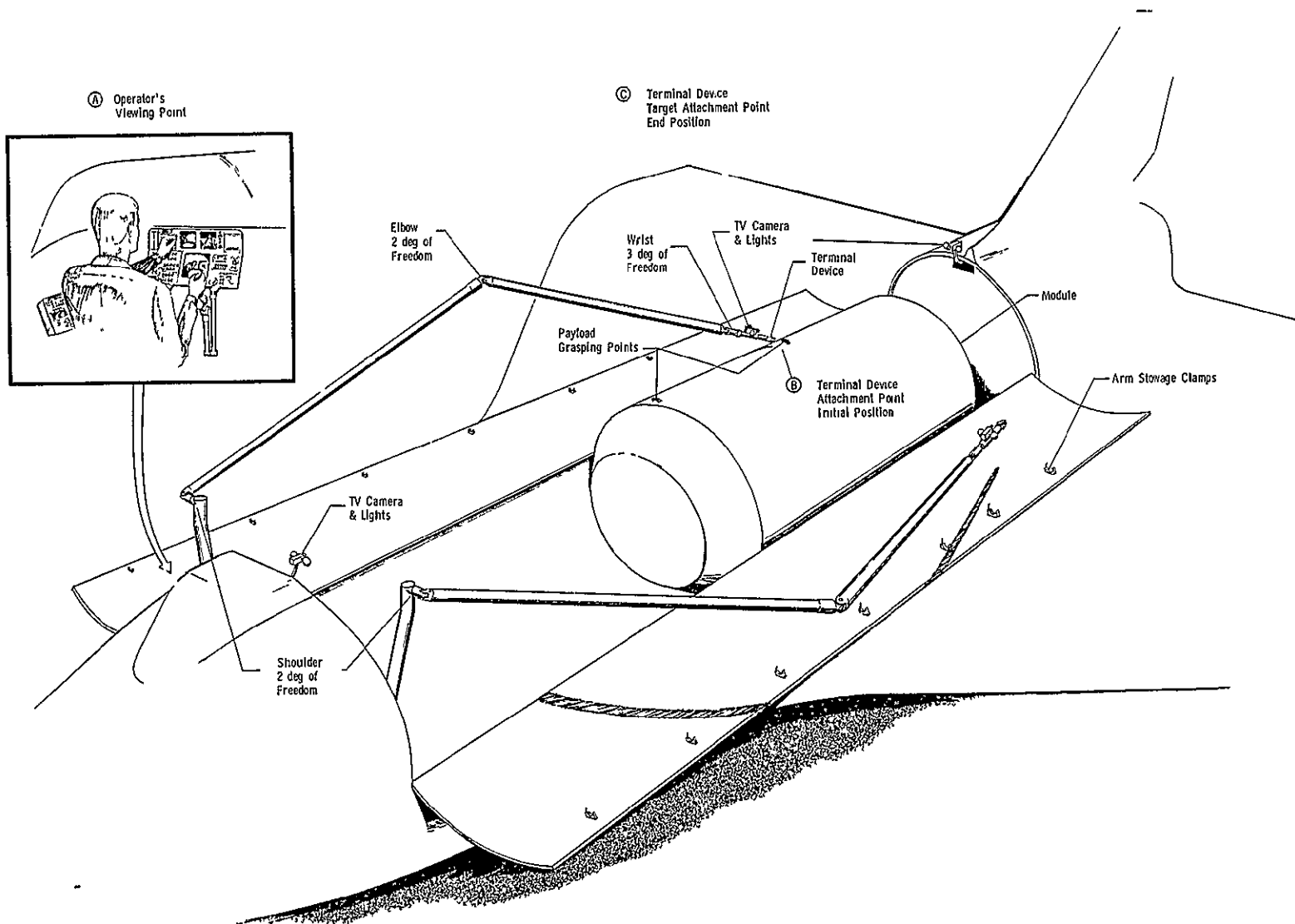


Fig. II-3 RMS Plane-of-Action

The 15-m(50-ft) reach distance of the manipulator arm within the plane-of-action defines one dimension of the work envelope. The out-of-plane motion of the end effector is dependent upon the controllability the pilot can maintain. Values for this bound can only be determined through simulation. However, realistic estimates can be made by determining what would be reasonable control bounds for the tasks to be performed. The maximum distance the terminal device will travel is 30-m (100-ft). A reasonable estimate of the out-of-plane motion bound for a 15-m (50-ft) manipulator arm is ± 3 m (± 10 ft).

The previous discussion was limited to the cargo transfer tasks. However, three comparable points can be nominally defined for each mission element with one exception. If there is any obstruction between the start and end points, the pilot will fly the problem in two sequenced planes-of-action to avoid the obstruction.

In summary, the work envelope is defined as a function of the task to be performed. Once the task is designated, a plane-of-action can be determined. The work within the plane-of-action is limited by the 15-m (50-ft) reach distance of the manipulator arm and the out-of-plane motion [± 3 m (± 10 ft)] by pilot controllability. All potential orientations of the plane-of-action are contained in the arm reach envelope (Fig. VII-9 of Report MSC05218).

III. CRITICAL SIMULATION REQUIREMENTS

A. DEGREES OF FREEDOM REQUIRED

In Section II.B, the character of all foreseeable forces and motion was itemized for the tasks associated with each mission element. A summary of the findings is contained in Table II-2. Examination of each of the columns in Table II-2 reveals that each of the mission elements can be regarded as involving a body A to which the manipulator arm is attached and a second body B (Fig. III-1) which is contacted and moved by the manipulator arm. In some cases, A represents the Shuttle alone (e.g., mission element No. 1), while in others, A denotes the Shuttle docked with

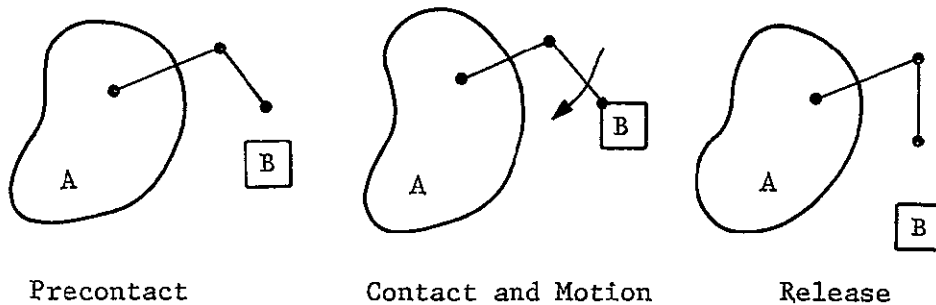


Fig. III-1 Dynamic Model for Mission Elements

some other vehicle (mission element No. 3). Body B ranges in size from small maintenance modules (mission element No. 6) to a large Space Station (mission element No. 2). The initial and final dispositions of B will vary from mission to mission. For example, during cargo transfer, the initial and final locations of B lie within body A, whereas, during payload retrieval, B is moved from without to within body A. Thus, it can be seen that the model shown in Figure III-1 is applicable (for analytical purposes) to all mission elements. To identify the model with a particular mission, one need only specify the proper initial and final conditions along with the pertinent inertia properties.

Having arrived at a dynamical model common to all mission elements, it is possible to discuss the dynamical aspects of a ground simulation without getting involved in a separate discussion for each of the mission elements.

First, with regard to the forces involved, one can conclude that forces and torques will act on both of the bodies, A and B, as well as the manipulator arm. These forces can be divided into two categories: the so-called active forces associated with the joint torques, and the inertia forces arising from the motions of the various bodies. During a simulation, duplication of active forces associated with a particular mission in space can be obtained by providing the proper torque motors for the manipulator. Duplication of the inertia forces can be guaranteed by providing the proper combination of inertia properties and freedom of motion for the bodies involved. Assuming any combination of inertia properties is available, it is necessary to determine what constitutes the *necessary* freedom of motion (or degrees of freedom, DOF) that must be provided to ensure a valid simulation.

Using the model shown in Fig. III-1, it can be seen that it would be *sufficient* to provide six DOF for body A and six DOF for B (the details of the motion of B relative to A being determined by the constraints associated with the manipulator arm). Hence, twelve DOF are sufficient for a valid simulation, but all of these may not be necessary.

If one assumes that the motion of A in inertial space need not be "seen" during the simulation, it is reasonable to investigate under what conditions one can eliminate the motion of A without degrading the fidelity of either the forces involved or the motion of B relative to A. An analysis dealing with this question is presented in Appendix A and the results are: It is possible to eliminate the three translational DOF of body A without fidelity degradation of the forces or the relative motion of B to A if, during the simulation, the mass of B is chosen in accordance with

$$m'_B = \frac{m_A m_B}{m_A + m_B} \quad \text{[III-1]}$$

where m'_B is the mass of B to be used during a simulation, and m_A and m_B are the actual masses of A and B during space operation. The foregoing conclusion is dependent upon the condition that the manipulator arm is massless. It was shown that

the mass of the manipulator arm has only a small influence on the motion of the system in space and hence, very little error is introduced by considering the manipulator to be massless. Therefore, it was determined that with proper mass adjustments, the three translational DOF of body A (the Shuttle) could be eliminated during a ground simulation.

Having shown that the translational motion of A could be eliminated, without appreciable error, by adjusting the mass of B, it is reasonable to ask whether or not the rotational motion can be eliminated by a similar adjustment in the moments of inertia of B. The analysis necessary for this determination is considerably more involved and was not performed as part of this study. Instead, a conservative estimate of the error involved in fixing the rotational motion without any adjustment in inertia properties is presented in Appendix A, with the following results: For small payloads, the rotational motion of the Shuttle can be eliminated without any adjustment in the inertia properties of the payload. (What constitutes a small payload requires further analysis, but it is estimated that those with masses of the order of the manipulator mass can be considered small.) For the larger payloads, some form of compensation is required. The necessary compensation might be obtained by proper adjustment of payload inertia properties, or by computer augmentation, or both. The computer augmentation would provide the proper "feel" by monitoring the relative motion of B to A, calculating the necessary torque compensation, and relaying the necessary signals to the operator's control mechanism.

Although not mentioned in Appendix A, an implicit assumption made in arriving at the conclusions pertaining to the rotational motion is that the initial angular velocity of the Shuttle is zero. If this were not the case, gyroscopic effects would enter the problem resulting in additional forces and torques in the system. If these effects are found to be appreciable, it would be necessary to provide rotational motion for the Shuttle.

To summarize, it is possible to eliminate the three translational DOF of the Shuttle by adjusting the mass of the cargo in accordance with Eq [III-1]. When the initial angular velocity of the Shuttle is not appreciable, it is possible to eliminate the rotational motion of the Shuttle by providing the proper torque compensation. Appendix A presents a more detailed analysis of this subject.

B. ORIENTATION OF TASK IN SIMULATOR

In Section II.C on the work envelope, it was concluded that for each RMS mission element a plane-of-action could be defined. The terminal device translates in the plane-of-action within the controllability bounds. However, the manipulator arm elbow moves in and out of the plane-of-action as a function of the specific task being done. The plane-of-action is defined by:

- 1) Operator's viewing point;
- 2) Terminal device attachment point when the target is in the initial position;
- 3) Terminal device attachment point when the target is in the end position.

The question to be considered is: What should the orientation of the plane-of-action be in a simulator? Two factors to consider are the effects on operation of the full size manipulator arm in the one-g environment and the simulator designs.

To introduce the manipulator arm structural bending characteristics as realistically as possible, it is desirable to have the arm segment motion aligned normal to the gravity vector. This should minimize any erroneous effects on bending characteristics resulting from operating in a one-g environment. This rationale indicates that the Shuttle should be oriented in a simulator facility so the RMS plane-of-action for each task corresponds to the horizontal plane. Therefore, for most tasks the Shuttle would be on its side or near that orientation.

In considering the effect on simulator design due to orientation of the plane-of-action in the simulator facility, it is necessary to realize that most simulators that can be used for the RMS application can be designed more easily to provide large, translational motion in two, rather than in three dimensions. Also, simulator cost is considerably lower. This point is observed readily by reviewing the potential simulation methods discussed in Chapter IV. In addition to the fact that simulators can be designed more readily for nominal planar operation, some simulators dictate a restriction on the orientation of the planar operation. An obvious example is an airpad simulator where the planar motion must be in the horizontal plane. In this example, the Shuttle would nominally be oriented on its side.

It can be concluded that for some simulation methods both the effects on manipulator arm operation and simulator design will dictate a horizontal orientation of the plane-of-action. For those cases where there is a contradiction on orientation, further tradeoffs will have to be performed.

Another consideration to be studied and considered in task orientation in a simulator is the effect on the RMS operator. The primary display of RMS position and motion is direct viewing by the operator. The operator, however, will not have sufficient windows to view the entire reach envelope or the areas obstructed by cargo or other modules as would frequently occur during cargo transfer. Therefore, a TV indirect viewing system will also be required to control the RMS.

If the Shuttle is oriented on its side for RMS simulations, then the operator's control station should be oriented similarly in order to align the coordinate system of the RMS with that of the operator for direct viewing. However, this orientation produces static vestibular/visual interactions that have experimentally been shown to degrade visual alignment tasks. Therefore, design considerations will have to include a tradeoff between optically rotating the visual field and orienting the operator on his side.

Optical rotation has several drawbacks in terms of intersensory discordance between what is visually perceived, what is actually known, and what is perceived through other psycho sensors. For example, for a rotated field of view, if the pilot can detect any reference of real world vertical, he will bias his perceived vertical control axis towards the real world vertical. This effect will degrade visual alignment tasks. In other words, the operator tends to mentally model his world based upon all inputs of logic, memory, vestibular, and visual cues. Any disparities between these cues are apt to distort this mental model about one or more axes, thereby degrading the operators control performance. This degrading is different for different individuals and is not readily alleviated with extensive training. Moreover, if the simulator is to be used for training of Shuttle crews, the transfer of learning between the simulator and the Shuttle will also be degraded. If the field of view is rotated, the mockup should be painted with highly reflective paint and the simulator covered with flat black paint and curtains, in order to minimize any reference to the real world vertical.

Orientation of the man on his side is an unnatural and uncomfortable position for the operator. It is not known to what extent the operator's visual aligning capability will be degraded because

of the intersensory discordance between the visually and vestibularly perceived orientation cues. Transfer of learning is also suspect if the operator is rotated onto his side.

In summary, if the Shuttle is oriented on its side, orientation of the operator should be an important design consideration. More is known about the effects of rotating the field of view than is known about the effects of orienting the operator on his side. Therefore, without further investigation, the more conservative approach would be to rotate the field of view and remove any visual cues of real world vertical from the window field of view. Optical system/alternatives for rotating the field of view are described in Appendix B. Orienting the operator on his side may create more severe intersensory discordance and would be uncomfortable and fatiguing.

IV. SIMULATION METHODS

The RMS space operations simulator must simulate the inertial reactions of the Shuttle, manipulator arms, and target as they interact with each other during each of the RMS missions. To achieve this condition in a laboratory, a state of weightlessness should be provided for the RMS and each vehicle, and friction should be eliminated in both translational and rotational vehicular motion. However, a simulation of this ideal state can only be approached. This should not be interpreted as indicating that RMS simulations are not worthwhile or practical. On the contrary, simulators are extremely vital to a manipulator technology program. The simulator provides a tool for investigation and verification of the RMS's concept and its operating procedures. The simulation will provide a means for refinement of system design and performance parameters.

Two modes of simulation capable of incorporating full size manipulator arms are;

- (1) the servo-driven mode and
- (2) the natural reaction mode.

In the servo-driven mode the target mockup is servo-driven so that its motion corresponds to zero-g space motion. This requires measuring the interaction forces and torques between the manipulator arm and the target vehicle and inputting them to a computer program that generates the servo positional commands. Actual vehicle mass and inertia properties are used in the computer program. This method does not require the target mockup to have full mass and inertia properties. Thus, this mode has the advantage of easily varied and accurately reproduced mass and inertia properties. The dimensions have to be full size because the target must interface with a full size manipulator arm. However, only portions of the target vehicle need be mocked up. In addition, the target mockup's center of rotation in the simulator does not have to coincide with the actual target vehicle cg location. Since only relative motion between the manipulator arm and the target vehicle is important, a total of six degrees of simulator motion can be used to simulate the 12 DOF problem where both the Shuttle and the target move. This is a significant advantage of the servo-driven simulation mode. RMS parametric data can be recorded during a simulation directly from the computer output without any instrumentation required.

This allows a parametric tradeoff to be performed when evaluating RMS performance. Also, initial dynamic conditions can be established easily by varying pot settings in the computer. These advantages and disadvantages are summarized and compared to the natural reaction simulation mode in Table IV-1.

In the natural reaction simulation mode the 12 DOF problem can be reduced to a 6 DOF problem (i.e., the Shuttle motion is eliminated) without introducing appreciable error as was reported in Chapter III. To collect parametric data, instrumentation is required. In addition, separate mechanisms are required to establish initial dynamic conditions.

In simulating weightlessness in the natural reaction mode, the target vehicle mockup must be supported at its cg. This point of suspension must be translatable in the simulator, and rotation of the test vehicle must occur about this point. In addition, the dimensions of the target mockup must be actual size.

Several basic types of natural reaction simulators were studied in this contract along with the servo-driven simulator. These were:

- 1) Airpad;
- 2) Cable suspension;
- 3) Neutral buoyancy.

Each type of simulator that was investigated is discussed.

The same remote manipulator system design was used for the servo-driven, airpad, and cable suspension simulators. The neutral buoyancy method imposes certain unique manipulator arm design requirements to satisfy water immersion constraints.

The ground rules under which the simulation methods were studied were:

- 1) Capability must exist for incorporating a full size manipulator arm;
- 2) Limited to six degrees of simulated freedom on target (i.e., no Shuttle freedom);
- 3) Maximum payload was a cylindrical module--

length ~ 18.3 m (60 ft),
diameter ~ 4.6 m (15 ft),
weight ~ 29,400 kg (65,000 lb).

Table IV-1 Comparison of Servo-Driven and Natural Reaction Simulation Modes

| TRADEOFF CHARACTERISTIC | SIMULATION MODE | |
|---|--|--|
| | SERVO-DRIVEN | NATURAL REACTION |
| Degrees of simulator freedom required to simulate Shuttle and target vehicle motion | Six degrees (relative motion) | Six degrees (relative motion) |
| Target mockup mass and inertia properties | Can use significantly reduced values | Must use actual values (An exception to this is discussed later.) |
| Target mockup dimensions | Must be full size (can use partial mockup) | Must be full size (Possible exception is neutral buoyancy.) |
| Location of target mockup center of rotation | Does not have to be at cg location of actual vehicle | Must be at cg location of actual vehicle |
| Data collection | Parameters are accessible in computer output | Requires added instrumentation to collect parametric data (not easily done for all parameters) |
| Dynamic initial condition | Easily varied in computer program | Requires a separate mechanism to establish them |

A. AIRPAD (SIX DEGREES OF FREEDOM)

1. Description

The airpad, six degree of freedom simulator is a natural reaction mode type. The simulator consists of airpads, air cylinder, and gimbals. In Figure IV-1, the simulator is shown conceptually as it would be used to study the task of cargo transfer.

The simulator, including target mockup and simulator structure, floats on three airpads mounted on a triangular base structure. This results in two translational degrees of freedom in the horizontal plane and one rotational degree of freedom (yaw) about the vertical axes.

An air cylinder is used for the vertical balance mechanism. The air cylinder provides natural reaction vertical travel by providing a vertical upward force equal to the combined weight of the gimbal structure and the target mockup. The air cylinder rides in vertical guides that are mounted to a vertical support structure.

The target mockup is suspended from the air cylinder in a two-gimbal structure giving two more degrees of rotational freedom (pitch and roll). The gimbals operate in a natural reaction mode. This requires a critical balance of the mockup in the gimbal system. Also, the gimbal support bearings must have very little friction. A spherical bearing could be used in place of the gimbals.

2. Task Orientation

As can be seen in Fig. IV-1, the Shuttle has been positioned on its side in the airpad simulator. This results in a horizontal orientation of the plane-of-action. The large travel requirements of the work envelope [15m (50 ft) x 30 m (100 ft)] are provided for by motion of the simulator on the airpad bearing surface. Clearance space around the simulator bearing surface was provided to allow the large target to move to the extreme of the work envelope. The small travel requirement [6m (20 ft)] is provided by the air cylinder. The air cylinder was somewhat higher than 6 m (20 ft) to accommodate the rotation of the mockup. This orientation was chosen because it is considerably more difficult to provide large travel capability with the vertical air cylinder mechanism than with the air bearing surface.

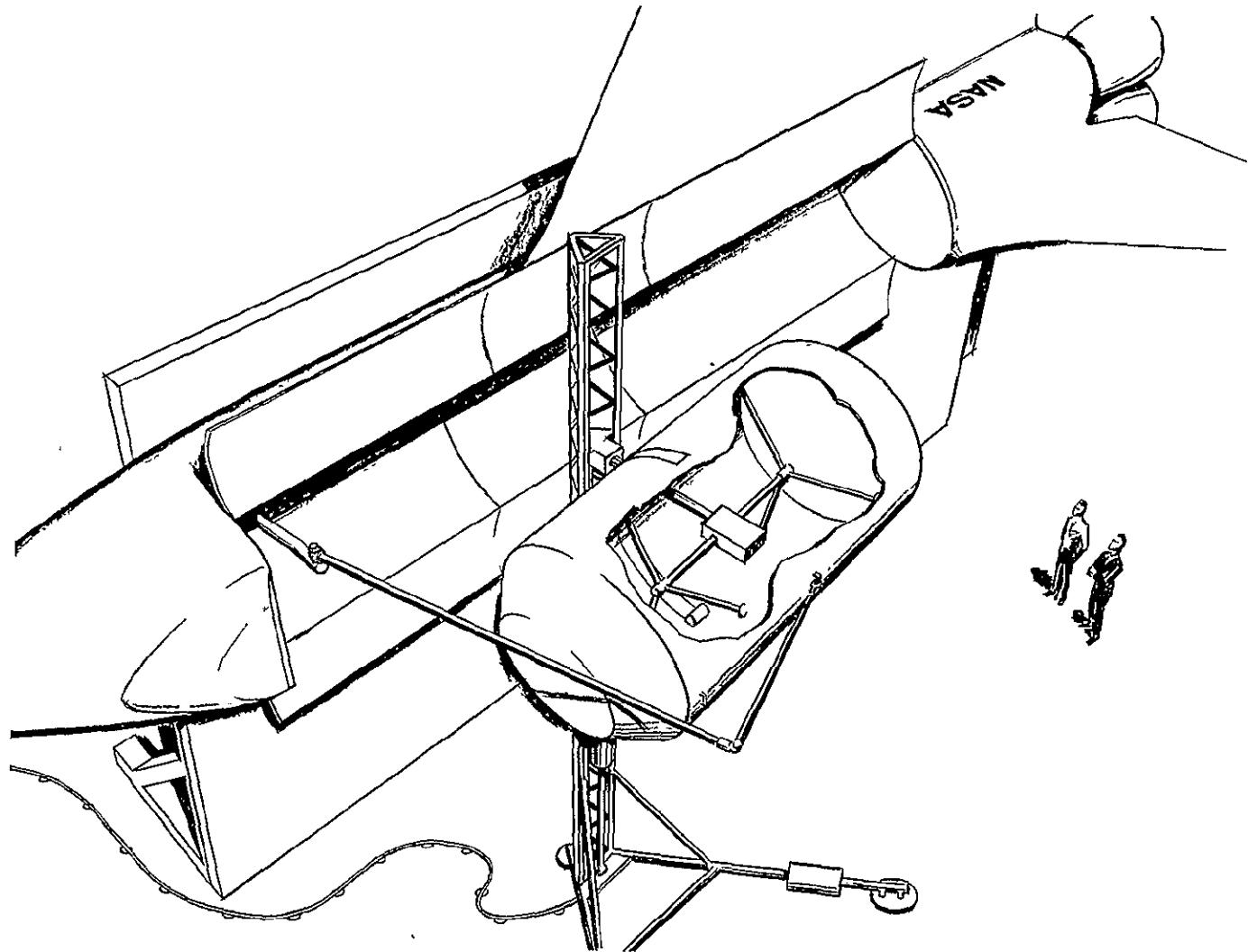


Fig. IV-1 Airpad - Six Degrees of Freedom

3. Design Considerations

Type of Airpad. Two basic types of airpads are available: one type contains a blower on the simulator base and operates on a large volume of air at low pressure; the other type operates on a small volume of air at high pressure. The latter requires a high pressure air hose hookup to the simulator base whereas the former requires only an electrical hookup and has a relatively larger air space between the airpad and the floor. Although the low pressure system appears to be the more practical, other features should also be considered in a tradeoff between the two types.

Levelness and Smoothness of Airpad Floor. Levelness and smoothness of the airpad floor are very critical. Specific requirements are dictated by the type of airpad used. A low pressure airpad does not require the floor to be as smooth as a high pressure pad does. If the floor is not level and smooth, the airpads will drift towards the low area in the floor and/or will encounter drag and buffeting with motion. Tradeoffs should be made to determine if periodic leveling and/or resurfacing are necessary. Poured epoxy floors are more economical, but another layer of epoxy must be poured if resurfacing is required.

Drag Effects. An airpad design that minimizes drag effects should be considered. Drag forces due to air hose supply lines (is used) and instrumentation lines can be minimized by using a series of small support airpads distributed along the lines.

Gimbal Balance Mechanism. Balancing of the two degree of freedom gimbal is critical. Since the gimbals are the natural reaction-type, torques arising from unbalanced conditions can cause the target mockup to rotate. Balance mechanisms should be provided to balance the target mockup in the gimbal system to eliminate this type of erroneous motion.

Gimbal Configuration. The design of the gimbal configuration must consider interference between the RMS terminal device and the gimbal structure. The gimbal structure must allow for maximum unobstructed mockup surface area. Since one attachment point on a module is midway along the side of the cylinder, this region cannot be obstructed by the gimbal structure. Therefore, an outer ring around the cylinder cannot be used to provide roll freedom.

The capture mission poses considerable restrictions on the gimbal configuration. It requires spinning the target mockup about one axis and providing at least a half section unobstructed mockup.

The gimbal configuration shown in Figure IV-1 appears to be very satisfactory. Pitch motion is obtained about a horizontal axis support from the air cylinder; roll is the innermost gimbal. This configuration requires a slot around the midsection of the mockup for roll clearance of the pitch gimbal support structure. However, the slot can be closed with a series of sliding panels which will individually open or close a small portion of the slot. A method must be provided to open each panel as it approaches the pitch gimbal shaft and to close it as the shaft is passed. This can be accomplished with a fixed cam or plow shear, but the mechanism should ideally be designed so that its motive power is supplied independent of the gimbal system.

Air Cylinder Design. The lifting force required in the vertical direction to counterbalance the gravity load is supplied by a piston and cylinder. The system pressure must be maintained constantly to provide a constant lifting force independent of piston inside the cylinder. There are basically two approaches that could be taken: one to provide a precision regulator to maintain constant pressure in the cylinder as the volume changes; the other to couple the cylinder to a total system volume (i.e., large air supply reservoir) large enough so that the change in system volume created by displacement of the piston to the extremities will be small, and the resultant pressure change will be acceptable. The design of either of these approaches represents a difficult design barrier for the RMS applications.

Vertical Guide Mechanism. Since the combined mass of the target mockup and gimbal system produces a large torque on the air cylinder, design of a guide mechanism for the air cylinder is extremely critical. It is necessary to design the guide mechanism so that the load torque can be reacted without restricting the vertical motion of the air cylinder. One way to accomplish this is with air bearings riding on vertical tracks inside the vertical support structure. The bearing surfaces should have considerable lever arms to react the load torque efficiently.

Location of Target Mockups cg. The location of the mockup cg must be at the intersection of the roll and pitch gimbal axes. (See Appendix C for details.)

Location of Simulator cg. The total simulator cg must be on a vertical line through the cg of the mockup; otherwise yaw motion will not occur about the mockup's cg. (See Appendix C for details.)

Mass and Inertia Distribution Between Target Mockup and Simulator Structure. Since the combined mass to be moved in the horizontal direction differs from that to be moved in the vertical direction, the total mass of the target cannot be divided between the target mockup and the simulator. Therefore, the simulator mass must be made as small as possible as compared to the target mass. (See Appendix C for details.)

Location of Vertical Guide Mechanism. The vertical guide mechanism shown in Fig. III-1 is located to the side of the mockup. The ideal location would be below the target mockup cg. However, locating it below the mockup cg results in a difficult mechanical design problem. The guide mechanism must have a telescoping device. This type of mechanism is not easily designed to meet a requirement of negligible expanding and closing forces. Since the telescoping mechanism requires a vertical force for both up and down motion of the simulator, the air cylinder could not be used to supply the force because it is unidirectional.

Counterweights on Simulator Base. Since the vertical mechanism will have considerable mass, counterweights will have to be added to the forward airpad legs so that the simulator cg will be located below the target mockup's cg.

B. CABLE SUSPENSION

1. Description

This natural reaction simulator (Fig. IV-2) consists of a crane, a gimbal system and a vertical balance mechanism.

The gimbal system is supported by cables from an overhead servo-driven crane. The cables are attached to counterweights. Thus, natural reaction vertical motion is theoretically provided.

Lateral and horizontal translation in the horizontal plane is provided by allowing small displacements of the target mock-up from vertical. Sensors provide off vertical errors that are used to servo the crane. Thus, the mockup is kept near the vertical position at all times. This should minimize pendulum effects and provide a natural reaction response.

The two degree (pitch and roll), natural reaction, gimbal system configuration used for this simulator is the same as the one for the six degree of freedom airpad simulator discussed previously. Yaw motion is provided by a bearing surface where the gimbal structure attaches to the cable rigging.

2. Task Orientation

The task orientation used for the cable suspension simulator (Fig. IV-2) is with the Shuttle on its side, (i.e., horizontal orientation of the plane-of-action). The 30 m (100ft) requirement of the RMS work envelope would be provided by the longitudinal track. The lateral track would provide the 15 m (50 ft) requirement. Considering the fact that the maximum size module is 18 m (60 ft) long, there are two options on the length of the lateral track: one to make the track 24 m (80 ft) in length, allowing the end effector to travel 15 m (50 ft) when the long axis of the module is parallel to the lateral drive; the other option would be to support the right longitudinal track in a manner that allows passage of half of the module underneath. Then the lateral track would be 15 m (50 ft) in length; vertical travel would be 6 m (20 ft). However, the height of the overhead crane above the floor would be considerably more than the 6 m (20 ft) travel requirement because of the space required for the gimbal system, the cable suspension mechanism, and the counterweight system.

The task orientation with the Shuttle on its side was chosen to eliminate gimbal design problems that are inherent in a simulator configuration accommodating a vertical Shuttle orientation. For tasks like cargo transfer, the cargo module will nominally be rotated through 180 degrees about an axis normal to the plane-of-action. This gimbal travel requirement is easily provided with the gimbal configuration shown in Fig. IV-2. However, if the Shuttle were located in a vertical orientation below this same gimbal system, the 180-degree travel capability could not be provided because of a gimbal lock problem. A different gimbal sequence could alleviate the gimbal lock problem. This appears to be an obvious solution, but other gimbal configurations would result in considerable support structure obstructions to the

IV-10

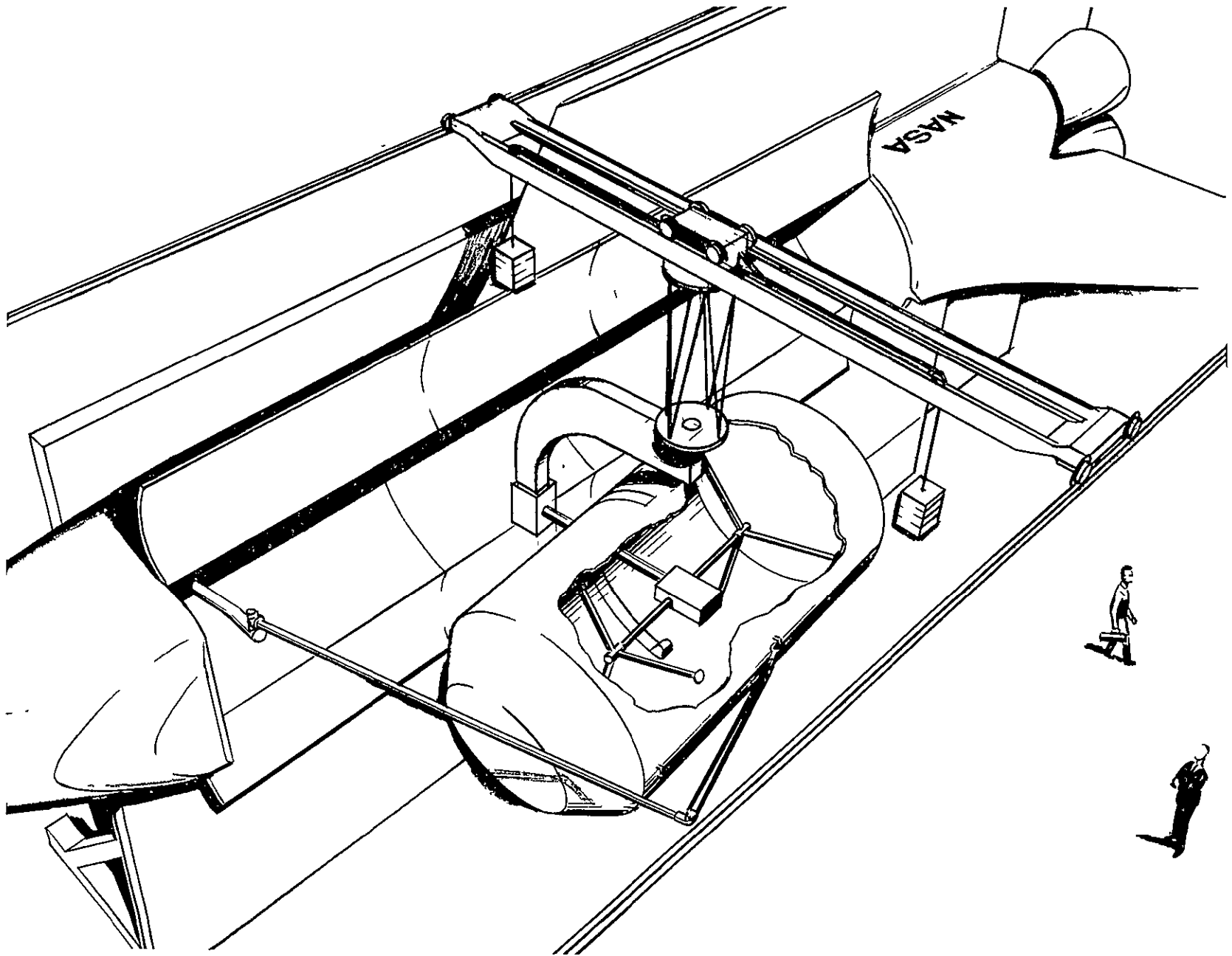


Fig. IV-2 Cable Suspension

target mockup, and the mechanical design would be more complex. Therefore, the cable suspension method has been baselined to the Shuttle-on-its-side orientation.

3. Design Considerations

Vertical Balance Mechanisms - The vertical balance mechanism has several significant design problems. The support cable rigging must be configured so as to minimize pendulum effects. However, it must also allow for a natural reaction motion around the vertical to horizontal forces. The length of the cables should also be considered.

The counterweights used to balance the combined weight of the target mockup and gimbal structure must be supported on separate booms from the crane's carriage. Space for the counterweights must be included on each side of the facility. The cable mechanism that routes the cables to the counterweights will not be simple. This is especially true because of the natural reaction requirement.

Vertical Sensors - Sensors like accelerometers or pendulums would have to be used to provide vertical information for driving the crane. Also, an azimuth (yaw) sensor would be required. The natural reaction functioning of the simulator with respect to horizontal forces would be questionable. This aspect of the simulation tends more toward a servo-driven technique.

Location of Target Mockup cg - The location of the mockup cg must be at the intersection of the roll and pitch gimbal axes.

Location of Simulator cg - Only the mass of the gimbal structure enters into the simulation. There is no restriction on the location of the gimbal system cg.

Mass and Inertia Distribution Between Target Mockup and Simulator Gimbal Structure - Since the combined mass (gimbal structure plus mockup) to be moved in all three translational directions is the same, the mass could be distributed between gimbal structure and mockup. However, the target mockup's orientation with respect to the gimbal structure changes; therefore, the inertia cannot be distributed. A tradeoff would have to be performed as to the effect on the inertia problem when mass is redistributed.

C. SERVO-DRIVEN

1. Description

The elements of the servo-driven simulation approach are shown in the information flow chart of Fig. IV-3 and the simulator configuration is shown in Fig. IV-4. The technique requires a six-degree of freedom servo-driven moving base, target and Shuttle mockups, manipulator arm, load cells, and a computer.

The manipulator arm is controlled by a pilot with direct view and television. Manipulator arm interaction forces and moments are measured by a set of load cells mounted either at the manipulator base or at the target mockup attachment point. The interaction forces and moments are input to a computer program containing the relative equations of motion for the Shuttle-target configuration. Vehicle characteristics such as inertia, mass, and control system torques can be introduced easily. The moving base is driven by positional servo commands from the computer, resulting in the proper motion between the manipulator arm and the target.

2. Task Orientation

The horizontal task orientation was chosen for the servo-driven simulator because the configuration results in a better mechanism design. The 30 m (100 ft) end effector travel requirement would be provided by the longitudinal drive, and the 15 m (50 ft) travel requirement by a 24 m (80 ft) lateral drive. The vertical drive travel would be 6 m (20 ft) if space could be provided below and above the work area to allow the module to rotate up to 60 degrees in pitch. Otherwise the vertical drive travel would have to be increased to accommodate this situation.

The Shuttle-on-its-side orientation minimizes the height of the vertical drive support pedestals: a considerable mechanical design advantage. The target mockup and gimbal structure is not cantilevered from a pedestal as it would be in other configurations. Finally, obstruction of the RMS work area by the simulator structure is minimized.

3. Design Considerations

A considerable design problem with a servo-driven simulator is the requirement for a rigid structure and a fast response servo. The servo system structure must be rigid to the extent that the lowest resonant frequencies of the structure are greater than the required response of the simulated vehicle by at least a factor of two.

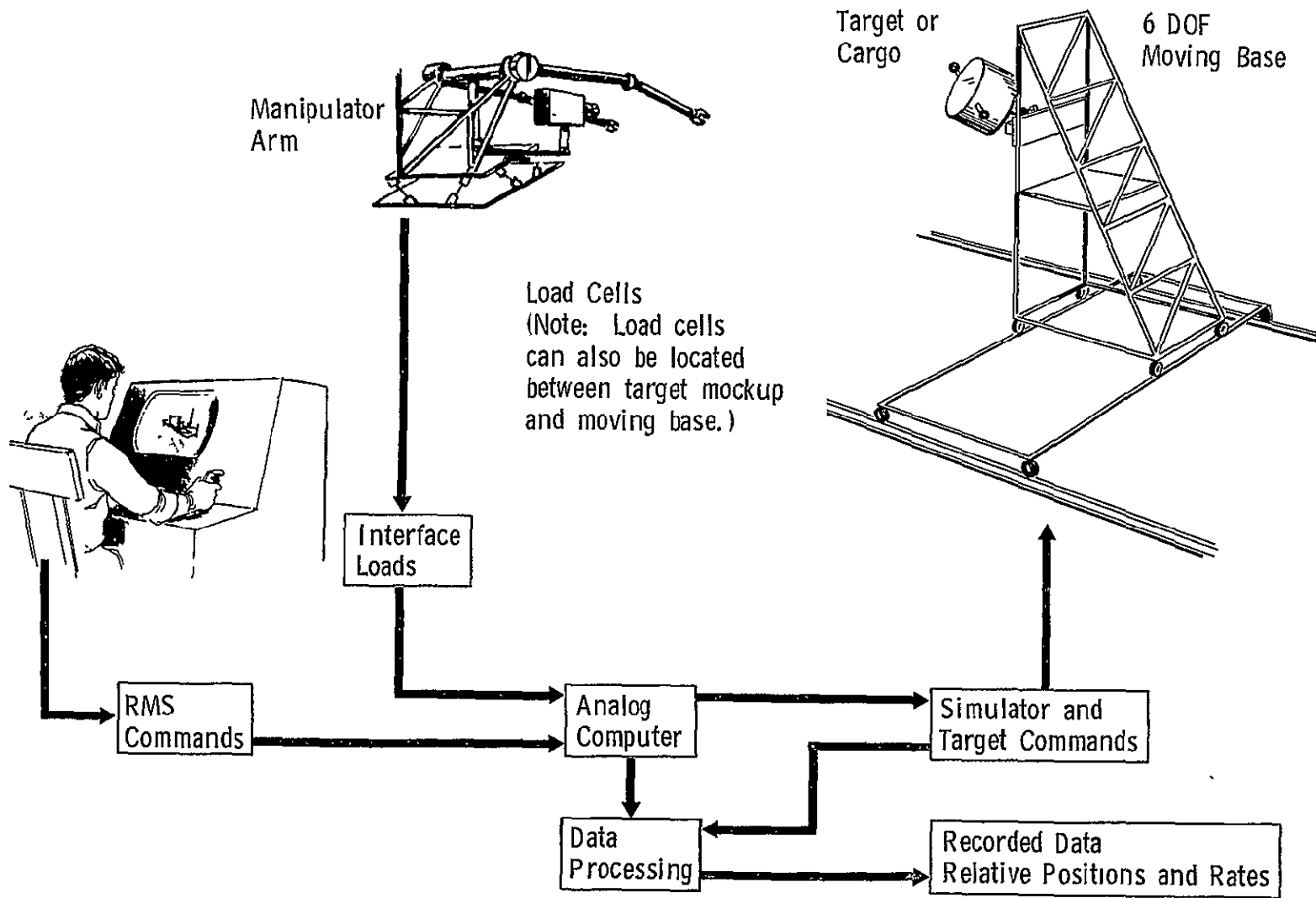


Fig. IV-3 Simulation Flow Chart

IV-14

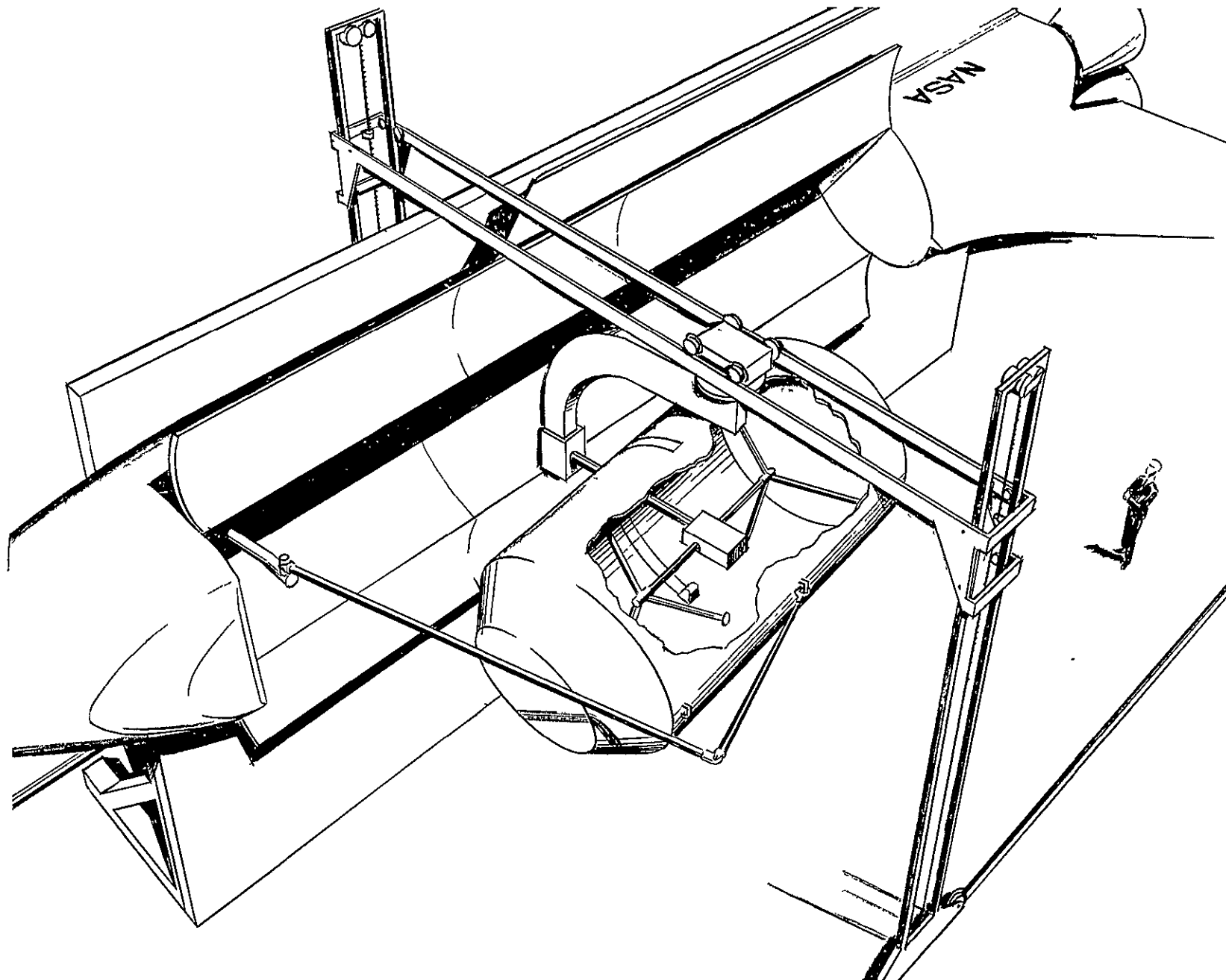


Figure IV-4 Seryo-Driven

D. NEUTRAL BUOYANCY

Neutral buoyancy simulations have been used extensively for crew training, crew compartment evaluations, crew capabilities, and crew task time line determinations. The advantages of using simulations include low cost operations, complete 6 DOF, and large volumes. Design considerations include safety, viscous damping, hydrodynamic inertia, visual degradations, difficulties in obtaining neutral buoyancy and corrosive effects of water.

1. Description

A neutral buoyancy facility approximately 49 m (160 ft) in diameter and 27.5 m (90 ft) deep would be required to simulate the complete work envelope of the RMS. (See Fig. IV-5.) However, the NASA MSFC facility currently includes the largest inland neutral buoyancy facility in existence, a 23 m (75 ft) diameter, 12 m (40 ft) deep neutral buoyancy facility. Figure IV-6 depicts use of this facility for RMS simulations. Positioning the Shuttle on its side (Fig. IV-7) allows use of a more shallow facility with less compressing of the neutrally buoyant cargo modules.

The basic system would include mockups of the Space Shuttle orbiter with cargo bay, RMS operator control station, docking port, and one 15 m (50 ft) manipulator arm. The arm would be nearly neutrally buoyant. Two or three neutrally buoyant cargo modules of various shapes and sizes would also be included. An overhead crane would be required to position a partial mockup of a space station if the cargo docking task were to be simulated. (However, MSFC's facility has only a 3 m (10 ft) hook height above the tank).

Options to the basic system would include a water filled control station for a neutrally buoyant and somewhat better evaluation of restraints and reaction forces for various control configurations but with an increase in the cost for hermetically sealed controls and displays. Therefore, it is suggested that layout and restraint evaluations be conducted under a separate neutral buoyancy investigation regardless of which simulation method is used.

Two 15 m (50 ft) arms would be another option for more realistic time lines in assembly and servicing tasks and for close-in camera coverage of cargo docking.

A larger facility would allow more of the operational envelopes to be included in the simulation. A coastal shoreline salt water neutral buoyancy facility, such as in the Virgin Islands, might be used for such a facility.

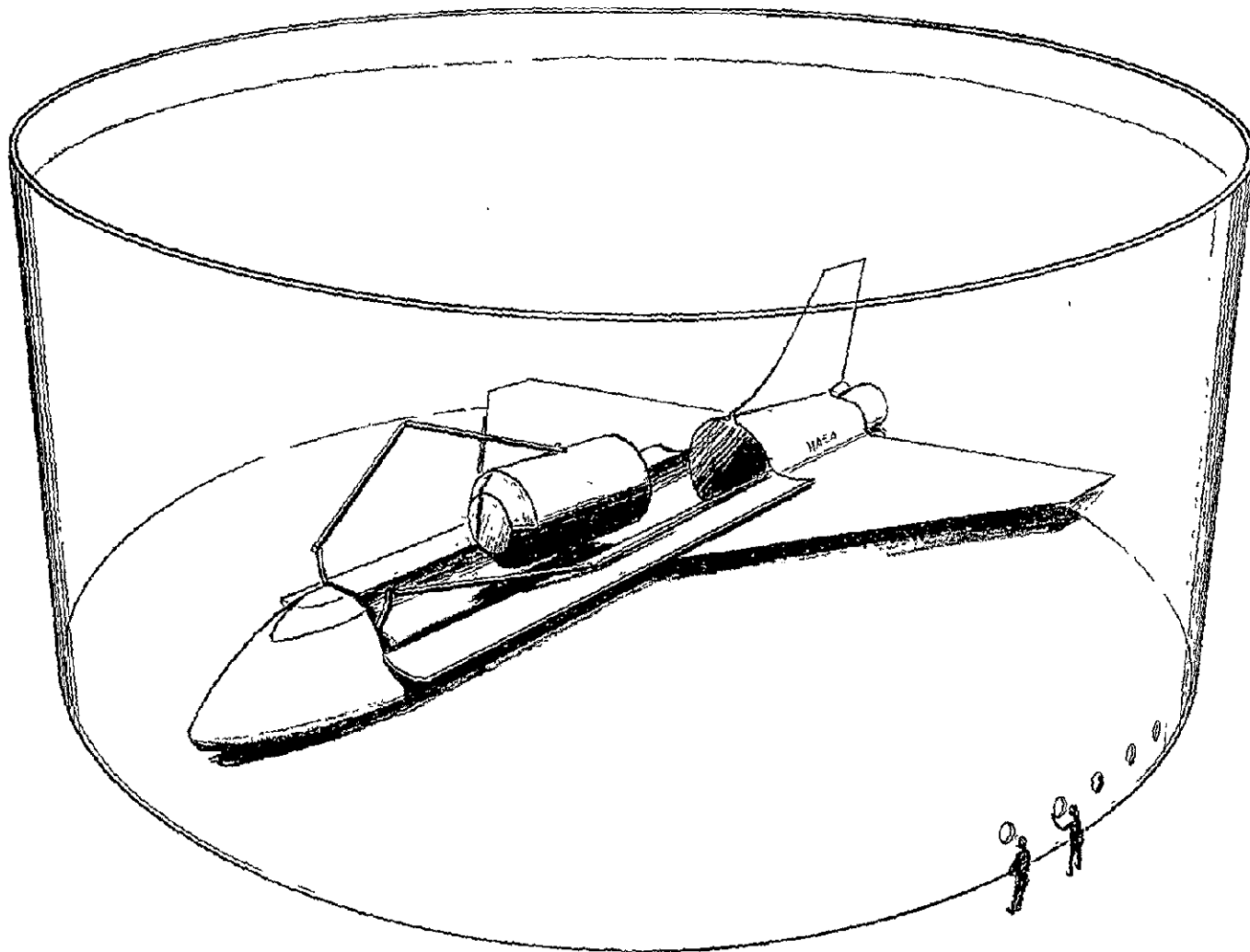


Fig. IV-5 Neutral Buoyancy Facility for Complete RMS Work Envelope

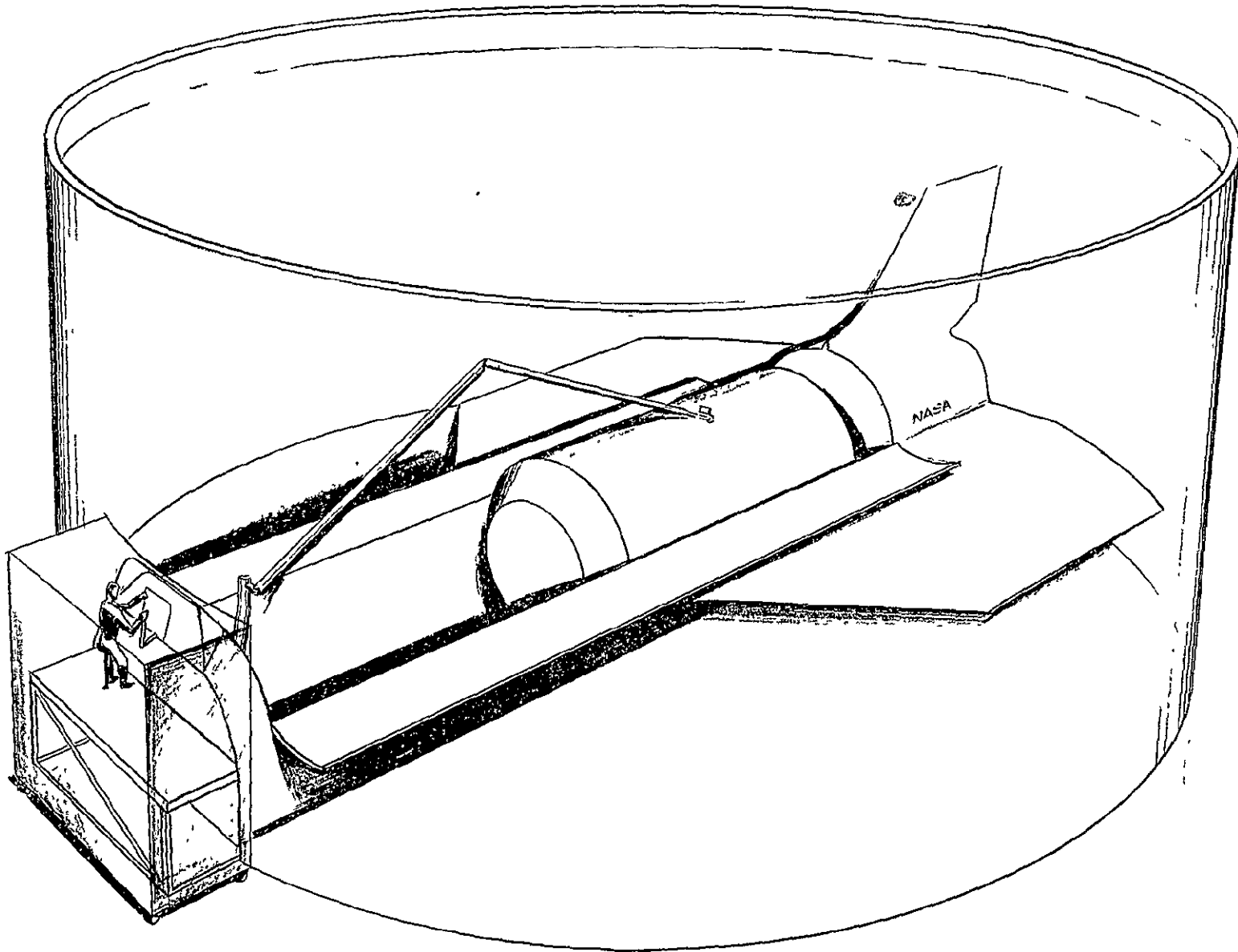


Fig. IV-6 An Adaptation of MSFC Facility for RMS Simulation

IV-18

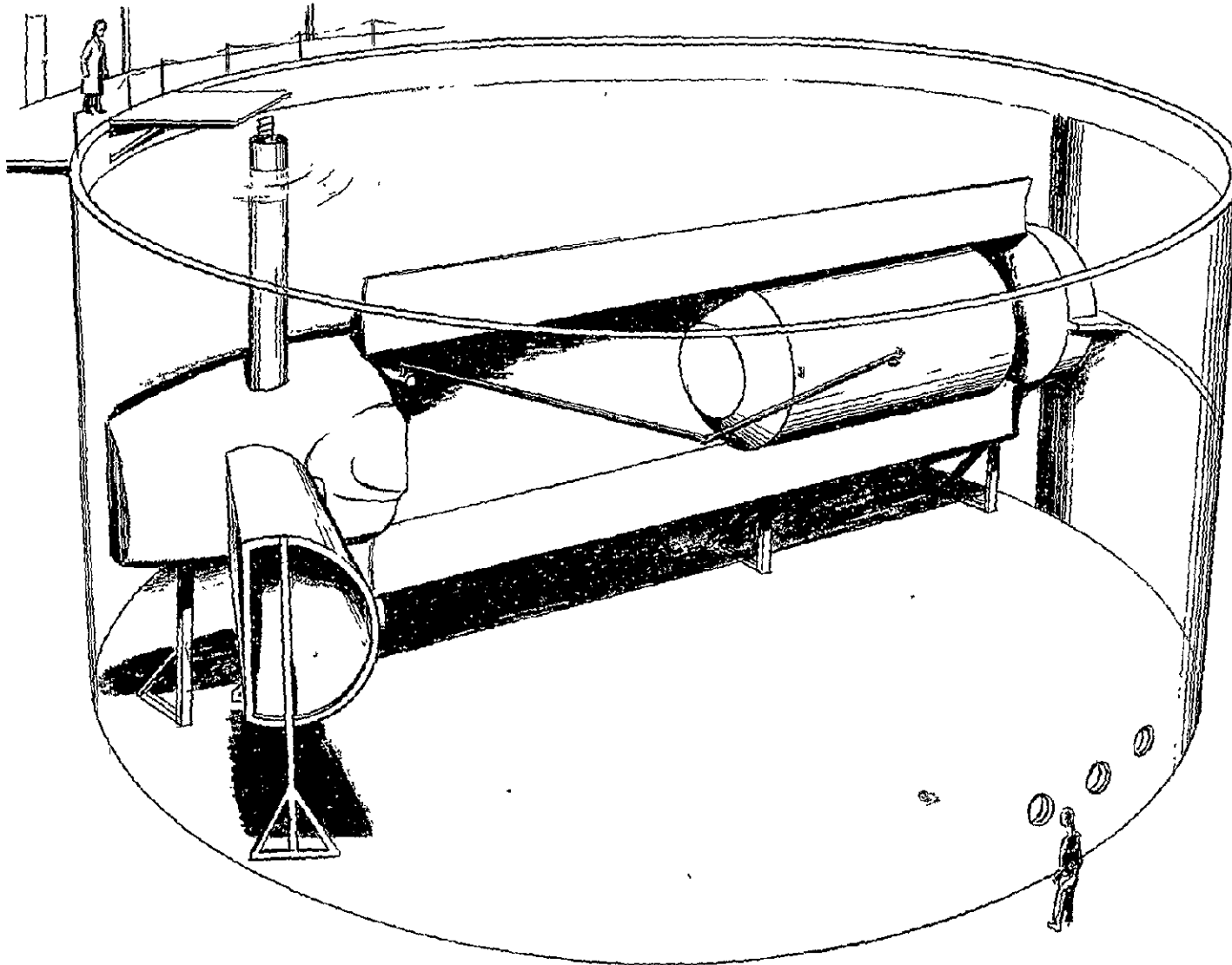


Fig. IV-7 Optimal Use of MSFC Facility for RMS Simulation

A gimballed cargo module or space station docking port would allow tracking and capture of a dynamically controlled target in from 3 to 6 DOF.

2. Task Orientation

Orientation of the Shuttle onto its side positions the plane-of-action in the horizontal plane. This has two distinct advantages: (1) changes in depth of cargo are minimized, and therefore, the range of compression forces on mockups will be minimized; (2) from a facility point of view, for the same volume of water, it is more economical to build a shallow neutral buoyancy facility than a deep facility.

3. Design Considerations

Neutral Buoyancy of Cargo Module Mockups - Extensive effort is required in order to locate the cg of the cargo module mockup coincident with the center of buoyancy (cg) and nearly coincident with the cg of the actual module. Moreover, the specific gravity of the mockup must be maintained sufficiently close to 1.0. Because of the vertical traverses involved, it is required that mockups are noncompressible in order to maintain a specific gravity sufficiently close to 1.0 throughout depth changes of up to 9 m (30 ft).

"Sufficiently close" is determined by the level of simulation fidelity required. For a given delta between the specific gravity of the water and that of the mockup, there will be a corresponding nonlinear acceleration either upwards or downwards of a nearly neutrally buoyant mockup. This acceleration is a function of volume and horizontal area of the mockup as well as the delta specific gravity. For example, for a mockup 127 cm (50 in.) long,² weighing 204 N (45.9 lb), with a horizontal area of 1.0 m² (9.1 ft²) and a specific gravity 0.001 less than water, it will have risen 0.305 m (1 ft) in eight seconds and 12.2 m (40 ft) in 50 seconds. If the delta specific gravity is 0.0001, it will have risen 0.06 m (0.2 ft) in eleven seconds and 3 m (10 ft) in 82 seconds. To maintain the specific gravity of water within 0.0001, the water temperature must be controlled within $\pm 5^{\circ}\text{C}$ or 0.9°F . However, temperature variations in large neutral buoyancy facilities are sufficiently small and pose no serious problems.

If the mockup is attached to the RMS arm, then the critical fidelity is one of force and is relative to the commanded forces. For example, the fidelity requirements may require that applied tip forces be within 10% of those required for actual zero-g

operations. In which case, for a 22.25 N (5 lb) tip force application, the vector sum of the hydrodynamic inertia, viscous drag, and the force resulting from a specific gravity delta would have to be less than 2.23 N (0.5 lb).

Natural Frequency Damping - A primary concern in the design of the zero-g RMS is the damping that may be required in order to adequately control the arms. The neutral buoyancy's water viscosity will damp out any natural oscillation of the arms. Therefore, a design consideration will be to produce an oscillation of the arm artificially in order to investigate controllability of the arm during oscillation.

Visual Limitations for Direct Viewing - The index of refraction of water is approximately 1.3 and for air approximately 1.0. The operator looking through air (either in goggles or a hermetically sealed crew station) into water will see objects that appear to be at a distance only 3/4 of the actual distance. Therefore, the object appears to be 33% larger than actual size. It is not presently feasible to overcome this magnification optically without severe vertigo and disorientation by the operator. The only feasible solution would be to reduce by 1/4 the length and size of the RMS arms, cargo modules, etc. There are, however, other visual problems associated with neutral buoyancy that cannot be so easily resolved. The visual field is limited by the 48.5° critical angle for total reflection of light passing from water into air. This limits the binocular field of view to 97° (normally 130° vertically and 200° horizontally). Present day wraparound goggles, although increasing the visual field, create illusions and vertigo and, therefore, are not recommended. Depth cues are more pronounced in water because of the severe light attenuation. Whereas in air it is often difficult to determine whether an object is small and close or faraway and quite large, in water the light attenuation facilitates this determination. Any motion or cloudiness of the water will increase the light attenuation as well as degrade resolution. Precise lighting levels and color are impossible to reproduce underwater. (The index of refraction is slightly different for different colors; however, the use of collimated lighting appears to improve color reproduction.) In summary, the RMS simulation would have to be 3/4 scale, depth cues would be more pronounced, and lighting levels would be very low fidelity.

Visual Limitations for TV Viewing - The 33% magnification problem of direct viewing could be resolved with appropriate lenses or with a 3/4 scale facility. The depth perception problems would be even more pronounced and lighting fidelity no better.

Mass and Inertia Limitations - Neutrally buoyant cargo modules and nearly neutrally buoyant RMS arms will be limited in mass, and therefore, inertia. The weight will be limited to 62.4 times the displaced or captured volume of water in cubic feet. Therefore, for some cargo module configurations the forces exerted by the arms per unit acceleration of cargo will be unrealistically low.

Dynamic Fidelity - Viscous drag, hydrodynamic drag, and planing are all dependent on the speed and direction of movement of an object through a liquid. Viscous drag requires an increased force in the direction of travel, opposes any velocities, and severely damps any oscillations in the RMS. The inertia of the mass of water which a moving object moves along with it is hydrodynamic inertia. The mass of water is quite different for different directions of movement unless the object is symmetrical in shape. Planing is also quite different for different directions of movement unless the object is symmetrical. Therefore, limitations require that all moving objects be symmetrical for acceptable fidelity of dynamics. Dynamics will be of low fidelity due to viscous drag and the empirical evaluation of arm oscillation control problems cannot be accomplished.

Safety Considerations - Consideration should be given to electrical and structural failures and their resultant hazards. These hazards, although complicated by the water environment, should pose no obstacles to man-rating of the facility.

Destructive Effects of Water - Considerations should be given to the protection of the mechanical and electrical subsystems from the corrosive and damaging effects of water.

V. COMPARISON OF SIMULATION METHODS

A. FACTORS OF COMPARISON

It is important to compare the capability of each simulation method for performing the RMS mission requirements. The impact of each simulation method on RMS design is also significant. Finally, the major design problems associated with realizing the desired design must be considered.

1. Dynamic State

The forces and motions that define the dynamic state for each mission element were presented in Chapter II. A summary of the capability of each simulation method for realizing the desired dynamic state is presented in Table V-1. In viewing Table V-1, it is worth noting that each of the simulation methods is presumed to be 6 DOF simulators and hence the degree to which they can realize the desired dynamic state is really no different than the degree to which the 12 DOF problem can be reduced to a 6 DOF problem. (See Chapter III for details.)

2. Work Envelope

The work envelope was defined relative to a task dependent plane-of-action in which the end-effector moved. (See Chapter II.) The bounds in terms of terminal device motion are a partial circle having a radius of 15 m (50 ft) in the plane-of-action and a controllability dependent out-of-plane motion of ± 3 m (± 10 ft). All potential orientations of the plane-of-action are contained in the wrist reach envelope. However, for most mission elements, the plane-of-action will be close to a vertical plane out of the Shuttle bay.

Each of the simulation methods has the potential capability of realizing these work envelope requirements. However, each method has unique design problems that are compared later.

Table V-1 Simulation Method Dynamic State Capability

| MISSION ELEMENT | SIMULATION METHOD | | | |
|-------------------------------------|-------------------|------------------|--------------|------------------|
| | AIRPAD | CABLE SUSPENSION | SERVO-DRIVEN | NEUTRAL BUOYANCY |
| 1) Unstowage and deployment | C | C | C | C |
| 2) Berthing Shuttle | C | C | C | C |
| 3) Cargo Transfer | E | E | C | E |
| 4) Deployment of payloads | C | C | C | C |
| 5) Retrieval | E | E | C | E |
| 6) Maintenance - Shuttle docked | E | E | C | E |
| 7) Maintenance - Shuttle not docked | E | E | C | E |

Note:

C - Simulator is capable of realizing the proper dynamic state.

E - Simulator is capable of realizing the dynamic state, but not without some error. The principal source of error is inability to reproduce the gyroscopic effects due to the system's initial angular momentum.

3. Simulator Degrees of Freedom

This study has shown (Chapter III) that the twelve degree of freedom problem (i.e., six degrees for Shuttle motion and six for target motion) can be reduced to a six target degrees of freedom problem (in most cases with negligible error). Therefore, the minimum degrees of freedom required to simulate the dynamic state is six. Naturally, each simulation method presented has taken advantage of the design simplification resulting from using the minimum number of degrees of freedom. Therefore, there is no difference between simulation methods on this point.

4. Orientation of Task in Simulator

In all four simulation methods presented in Chapter IV, it was concluded that the most advantageous task orientation from a simulator design consideration was with the plane-of-action aligned to the horizontal plane. For the airpad, cable suspension and servo-driven methods, a significant increase in simulator design complexity arises if other orientations of the task plane-of-action are used. The task orientation chosen allows the largest simulator travel requirements, dictated by the work envelope, to be provided by those simulator degrees of freedom that can be most easily and effectively mechanized. In the neutral buoyancy method, the depth of the facility is reduced considerably when the Shuttle is oriented on its side.

Orienting the task so the Shuttle is on its side introduces the problem of the RMS operator's orientation which was discussed in Chapter III. However, this problem is common to all four simulation methods; therefore, it does not impact the comparison of simulation methods.

5. Impact of Simulation Methods on the RMS One-g Design

If the operating orientation of the manipulator arm with respect to the gravity vector were different for some of the simulation methods, it could result in arm design requirements that were dependent on the simulation method. However, since the operating orientation of the manipulator arm is the same for all simulation methods, it does not introduce any RMS design factors of comparison. The neutral buoyancy simulation method introduces the unique requirement of manipulator arm performance in water.

6. Complexity of Simulator Design

Gimbal System. There are no significant design differences in the gimbal systems required for the airpad, cable suspension, and servo-driven simulators. The neutral buoyancy simulator does not require a gimbal system. However, extensive effort is required to locate the cg of the target mockup coincident with the center of buoyancy.

Translational System. The variation between the simulation methods in design complexity for the translational systems is significant. The large translational requirements of the work envelope are not readily realized. The cable suspension and servo-driven simulators require lateral tracks 24 m (80 ft) in length from which the target mockup is supported. The servo-driven simulator requires vertical drive pedestals [6 m (20 ft)] to support the lateral tracks. The support structure for these translational drive tracks must be rigid, and the servo responses fast. The lateral track support structure for the cable suspension simulator would have to be capable of supporting 58,800 kg (130,000 lb) (maximum load). The crane would have to be capable of lifting this same load.

A very large neutral buoyancy facility by present standards is required to satisfy the large work envelope requirements.

The airpad simulator requires a very smooth and level floor for two translational degrees of freedom. Poured epoxy floors can be constructed readily. However, if other types of floors were used, leveling mechanisms would introduce more complexity. The vertical motion freedom in the airpad simulator requires a complex mechanical design. In fact, for the maximum loads 29,400 kg (65,000 lb) it represents a design barrier as discussed in the following section.

7. Major Design Problems.

The airpad simulator has a very significant design problem in the vertical mechanisms for large loads. Air cylinder and associated guide mechanisms capable of supporting 29,400 kg (65,000-lb) loads cantilevered out at 2.4 m (8 ft) do not exist in any simulators. In fact, the loads that existing designs are capable of supporting are in the hundreds of pounds, not tens of thousands. Also, there appears to be no other practical method of providing natural reaction motion in the vertical direction as part of the airpad structure.

The major design problems with the cable suspension simulator are rigidity of the lateral track, performance of the horizontal drive loops, and pendulum effects inherent in the cable support system.

The neutral buoyancy method is limited by difficulties in achieving neutral buoyancy, limited mass capabilities, and visual problems.

The servo driven simulator has a very significant design barrier because of large translational requirements. The validity of the performance of this type of simulator is dependent upon structural rigidity and fast servo response in the drive loops. The solution of this problem for a simulator having a 24-m (80-ft) lateral track and 6-m (20-ft) vertical pedestals is not realizable within practical design limits. The servo-driven method is effective only when used with a simulator that has smaller overall dimensions, since only then can the rigidity and servo response necessary be realized within practical design limits.

8. Adaptability of Simulation Method to Investigating the Manipulator Arm Bending Characteristics

The airpad simulator is the only one that adapts effectively and readily to investigation of the manipulator arm's bending characteristics. By supporting the arm at the elbow and tip with an airpad pedestal, planar bending studies can be performed.

B. CONCLUSIONS OF COMPARISONS

A summary of the comparison factors previously discussed is presented in Table V-2. The results of this study were presented to MSC at a midcontract meeting. The objective of the meeting was (1) to review the results of the study and (2) to select the simulation method that showed the most promise. In reviewing the comparison results shown in Table V-2, it was concluded that significant differences between simulation methods existed in three factors: (1) complexity of simulator design, (2) major simulator design problems, and (3) adaptability to investigate arm bending characteristics. In reviewing the complexity of design and the design problems for each simulation method, it was observed that these factors are related to only one degree of freedom for the airpad simulator whereas the others are

Table V-2 Summary of Comparison Factors

| COMPARISON FACTORS | AIRPAD | CABLE SUSPENSION | SERVO-DRIVEN | NEUTRAL BUOYANCY |
|--|---|---|---|---|
| 1. Dynamic state requirements | Each method has the potential capability of realizing these requirements. | | | |
| 2. Work envelope requirements | Each method has the potential capability of realizing these requirements | | | |
| 3. Simulator degrees of freedom required | Six | Six | Six | Six |
| 4. Orientation of task in simulator | Shuttle on side | Shuttle on side | Shuttle on side | Shuttle on side |
| 5. Impact on RMS one-g design | ← The same → | | | Arms must be operable in water |
| 6. Complexity of simulator design | Low | High | High | Low |
| 7. Major simulator design problems | Air cylinder functioning and load carrying capability | Function of horizontal drive loops and minimizing pendulum effects. | Obtaining sufficient servo response and structural rigidity | Large volume and realizing adequate visual conditions |
| 8. Adaptability to investigate arm bending characteristics | Excellent | Poor | Poor | Poor |

related to three or six degrees of freedom. Also, the airpad shows the most promise for studying manipulator arm bending effects in reduced degrees of freedom.

Considering these facts the airpad simulation method was selected. An option for providing vertical travel in the airpad simulator was discussed. This option involved transfer of the vertical travel requirement from the target mockup to the Shuttle mockup (i.e., providing a capability for the Shuttle to move up and down). This method is described in Chapter VII.

VI. MANIPULATOR STRUCTURAL DESIGN ALTERNATIVES

The manipulator arm structural design for operation in a one-g environment is considered in this section. The primary factors that are investigated are the static deflection of the arm and determination of the arm stress to assure that the arm will support itself in the 1-g environment. Four basic approaches are investigated, and the advantages and disadvantages of each technique are presented. Joint design for 1-g operation of the RMS was not part of this study.

A. ZERO-G DESIGN

The first approach considered is to use the arm design for zero-g in a one-g environment. The design is modified to exclude the deployment stub, but otherwise is identical with the preliminary design (MMC report MSC-05218) which has a 20.32 cm (8 in.) diameter aluminum tube sized to deflect 2.54 cm (1 in.) under maximum tip load.

Because the fixed-end conditions no longer involve the bending and torsional flexibility of the stub section, it is possible to consider the arm as a single beam with varying stiffness rather than a chain of bending and torsional elements. By the area-moment method, the deflection of the arm at any point may be calculated as the moment of the M/EI diagram due to a given set of loads.

Considering first the deflection due only to the design loads, the loading diagram, and the resulting bending moment and $\frac{M}{I}$ diagrams are developed as shown in Fig. VI-1. The segment lengths (ℓ) and cross-sectional moments of inertia (I) are taken from the preliminary design previously developed.

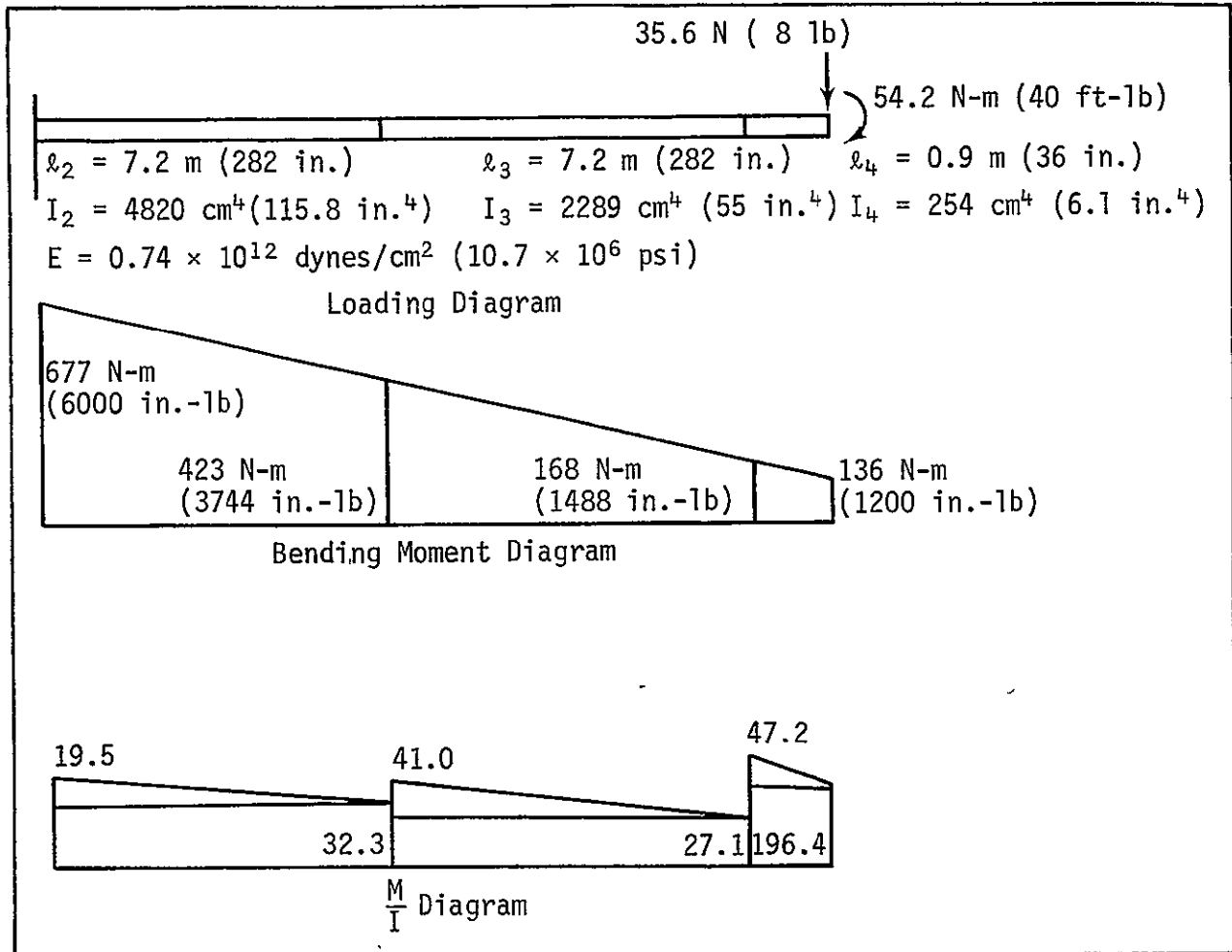


Fig. VI-1 Loading Conditions Due to Design Loads

The deflection is then calculated as

$$\delta_A = \frac{1}{10.7} \left[196.7 \times 36 \times \frac{36}{2} + 47.2 \times \frac{36}{2} \times \frac{2 \times 36}{3} + 27.1 \right. \\ \times 282 \left(\frac{282}{2} + 36 \right) + 41 \times \frac{282}{2} \left(\frac{2 \times 282}{3} + 36 \right) + 32.3 \\ \left. \times 282 \left(\frac{282}{2} + 282 + 36 \right) + 19.5 \times \frac{282}{2} \left(\frac{2 \times 282}{3} + 282 + 36 \right) \right] \\ = 2.02 \text{ cm (0.797 in.)}$$

Notice that this deflection is less than 2.54 cm (1.0 in.) because the deflection due to the stub section is not included.

Consider now the deflection of this structure including joint mechanisms under its own weight. The loading diagram and resulting bending moment and $\frac{M}{I}$ diagrams are shown in Fig. VI-2.

Taking $\frac{1}{E}$ times the moment of the $\frac{M}{I}$ diagram about point 4, the deflection due to the structural weight is found as:

$$\begin{aligned} \delta_4 = & \frac{1}{10.7} \left[\frac{1}{2} \times 88.5 \times 36 \times \frac{2}{3} \times 36 + \frac{1}{3} \times 38.4 \times 36 \times \frac{3}{4} \times 36 \right. \\ & + 14.1 \times 282 \left(\frac{1}{2} \times 282 + 36 \right) + \frac{1}{2} \times 368.2 \times 282 \left(\frac{2}{3} \times 282 + 36 \right) \\ & + \frac{1}{3} \times 548.6 \times 282 \left(\frac{3}{4} \times 282 + 36 \right) + 442.1 \\ & \times 282 \left(\frac{1}{2} \times 282 + 282 + 36 \right) + \frac{1}{2} \times 821.4 \times 282 \left(\frac{2}{3} \times 282 + 282 + 36 \right) \\ & \left. + \frac{1}{3} \times 614.9 \times 282 \left(\frac{3}{4} \times 282 + 282 + 36 \right) \right] = 40.7 \text{ cm (16.04 in.)} \end{aligned}$$

From the bending moment diagrams, the total bending moment at point 1 is:

$$\begin{aligned} M_1 = & 6000 + 31,105 + 17,122 + 135,219 + 34,074 = 25,610 \text{ N-m,} \\ & (223,520 \text{ in.-lb}) \end{aligned}$$

and at point 2 is:

$$M_2 = 3744 + 17,122 + 34,074 = 6200 \text{ N-m (54,940 in.-lb)}$$

and at point 3 is

$$M_3 = 1488 + 540 + 234 = 256 \text{ N-m (2262 in.-lb)}$$

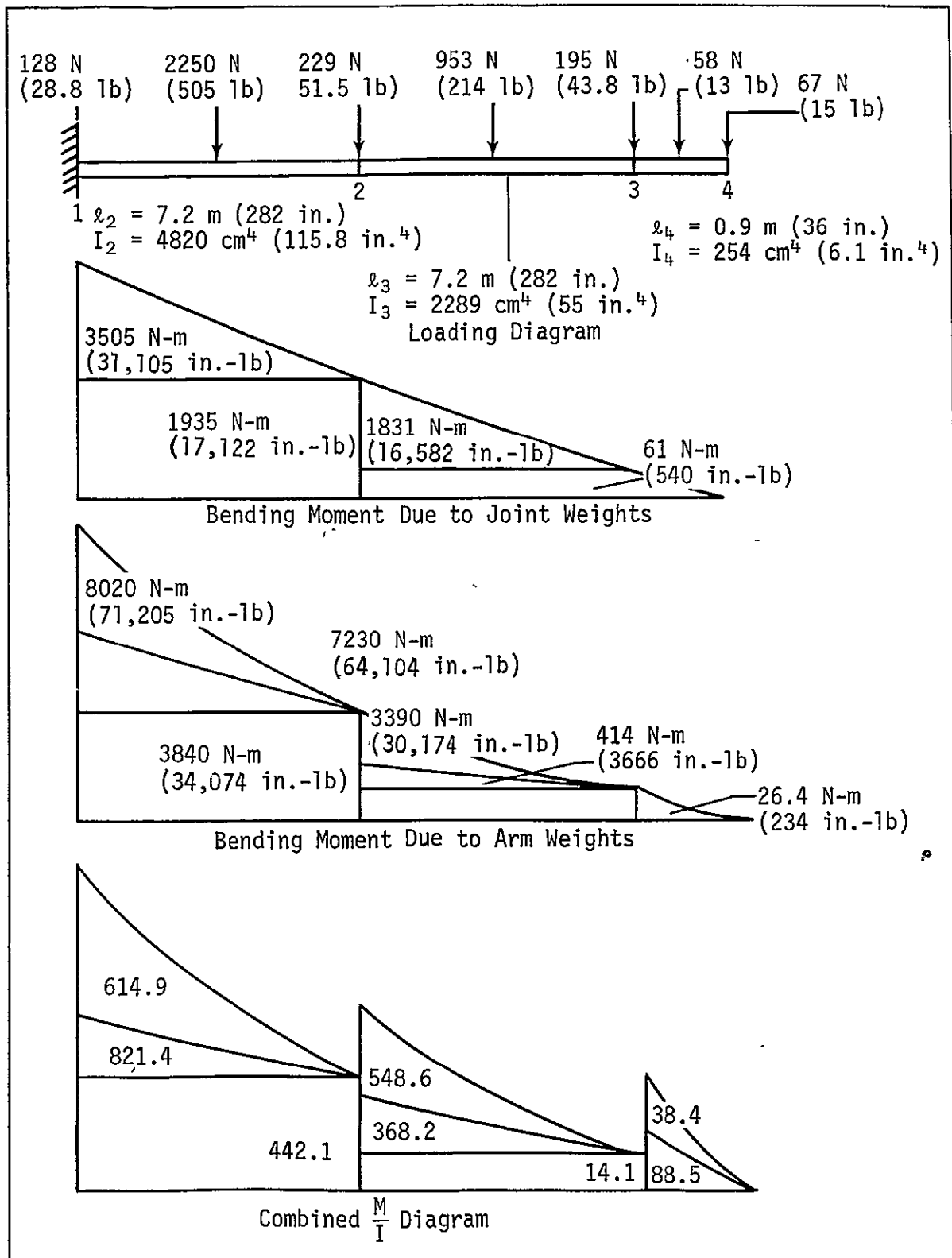


Fig. VI-2 Loading Conditions Due to Structure Weight

The corresponding bending stresses are

$$\sigma_1 = \frac{M_1 R}{I} = \frac{223,520 \times 4}{115.8} = 670 \times 10^6 \text{ dynes/cm}^2 \text{ (9721 psi) ,}$$

$$\sigma_2 = \frac{M_2 R}{I} = \frac{54,940 \times 4}{55.0} = 274 \times 10^6 \text{ dynes/cm}^2 \text{ (3996 psi) ,}$$

$$\sigma_3 = \frac{M_3 R}{I} = \frac{2262 \times 2}{6.1} = 51 \times 10^6 \text{ dynes/cm}^2 \text{ (742 psi)}$$

Since the allowable bending stress for structural aluminum alloys in tubing with $D/t \frac{8.0}{0.31} = 25.8$ is well over 4140×10^6 dynes/cm² (60,000 psi), the present structure is clearly adequate for one-g operation with considerable margin for handling loads. This means that the structural design for zero-g could be used for one-g operations and the tip force during cargo handling will cause a tip deflection similar to that which will occur in space. The disadvantage of this approach is that the arm tip will deflect an additional maximum of 40.6 cm (16 in.) in the vertical direction due to its own weight, and this tip deflection will be a function of the arm position.

B. STRUCTURAL DESIGN FOR ONE-INCH DEFLECTION

Consider now the problem of designing a structure similar to the present one but stiff enough to deflect only one inch in the vertical direction under its own weight plus design tip loads. It is clear that such a structure (assumed symmetrical) will deflect much less than one inch under design tip loads applied in any direction other than downward.

Since the total deflection of the present structure is 40.7 cm (16.04 in.) due to weight plus 2.02 cm (0.797 in.) due to design or 42.7 cm (16.84 in.), the simplest approach is to increase the stiffnesses of the sections by a factor of 16.84.

This, however, is not possible as stated, because any increase in E or I is accompanied by a change in weight, generally an increase. Among the common structural materials, an increase in E is accompanied by a proportional increase in density, which defeats the purpose.

For a given material, say aluminum, an increase in I may be obtained by increasing tube wall thickness, but again weight increases proportionately so the one-g deflection remains the same. The only remaining approach is to increase the tube radius, which increases I and also increases the weight but not proportionately, so that a decrease in tip deflection can be obtained.

Under reasonable assumptions that the weight of the joint mechanisms will increase in proportion to the weight of the arm sections, and stiffnesses of the sections increase in the same proportion, the tip deflection is proportional to weight per inch, and inversely to the EI, of the tube cross section. That is

$$\delta_4 = K \frac{Ae}{EI} = K \left(\frac{2\pi r t e}{E \pi r^3 t} \right) = \frac{2K}{(E/e)} \left(\frac{1}{r^2} \right)$$

where, as before,

r is the mean radius of the tube,

t is the tube wall thickness,

e is the material density,

E is the Young's modulus,

K is a proportionality constant.

Thus to decrease the one-g tip deflection from 42.7 cm (16.84 in.) to 2.54 cm (1.0 in.), the mean radius of all tubes must be increased by a factor of $\sqrt{16.84} = 4.10$. This is not exact since the 42.7 cm (16.84 in.) includes the 2.02 cm (0.797 in.) due to applied loads. This is a negligible error.

Increasing the mean radii of all tube sections by a factor of 4.10 will reduce the tip deflection under one-g to about one inch regardless of the tube wall thickness, which may then be chosen to limit tip deflection due to applied loads to one inch also, or to keep the bending stress down to safe levels.

The values of I have been chosen to accomplish this for minimum weight. However, if it is attempted to hold these values of I with the values of r increased by a factor of 4.10, the resulting wall thicknesses are impractically thin, e. g.

$$\frac{0.78}{4.10^3} = 0.0338 \text{ cm (0.0133 in.)}$$

It is essential to maintain the ratio $\frac{r_b}{r_a} = 4.10$ to limit the one-g deflection to one inch. It is assumed permissible to increase t to practical values which increases I. This has the effect of decreasing the tip deflection under applied loads to less than 2.54 cm (1.0 in.). It is also essential to keep the maximum stress less than the allowable stress.

The allowable stress is:

$$F_b = 62,000 \left[1.07 - 0.008667 \left(\frac{r}{t} \right) \right].$$

The bending moment at any point on the arm is directly proportional to the weight per inch. That is

$$\frac{M_a}{M_b} = \frac{r_a t_a}{r_b t_b}$$

and as shown before

$$\frac{I_a}{I_b} = \frac{r_a^3 t_a}{r_b^3 t_b}$$

$$\frac{\sigma_a}{\sigma_b} = \frac{M_a r_a}{I_a} \bigg/ \frac{M_b r_b}{I_b} = \frac{M_a}{M_b} \cdot \frac{r_a}{r_b} \cdot \frac{I_b}{I_a} = \frac{r_a t_a}{r_b t_b} \cdot \frac{r_a}{r_b} \cdot \frac{r_b^3 t_b}{r_a^3 t_a} = \frac{r_b}{r_a} = 4.10$$

Since the existing stress levels are quite low, 670×10^6 dynes/cm² (9721 psi), it is possible to increase them by a factor of 4.10 and still retain a sizable margin.

Let $\sigma_b = 4.10 \times 7721 = 1495 \times 10^6$ dynes/cm² (21,660 psi).

Assuming that the allowable stress should be at least 3450×10^6 dynes/cm² (50,000 psi).

$$F_b = 67,000 \left[1.07 - 0.008667 \left(\frac{r_b}{t_b} \right) \right] = 50,000$$

$$1.07 - 0.008667 \frac{r_b}{t_b} = \frac{50,000}{62,000} = 0.806951$$

$$\frac{r_b}{t_b} = 30.4$$

For arm section 1-2 $r_a = 3.61$

$$t_b = \frac{3.61 \times 4.10}{30.4} = 1.24 \text{ cm (0.49 in.)}$$

$$r_b = 3.61 \times 4.10 = 37.6 \text{ cm (14.8 in.)}$$

This says that in order to maintain a one-inch tip deflection under one g, the arm sections must be 75 cm (29.6 in.) in diameter with a wall thickness of nearly 1.27 cm (0.50 in.) for the upper arm section, and less for the forearm. This size presents mechanical problems for incorporation of the joint mechanisms, increased weight, and a system that does not have the same dynamical characteristics or appearance as the zero-g design.

C. TWELVE-INCH DIAMETER ARM SECTIONS

If the tube size of the outer arm sections are allowed to be twelve inches outside diameter, it is to be expected that for the same stiffness I_2 , I_3 , I_4 the tube wall thickness will decrease. This permits the same deflection under the design loads in orbit but less deflection under one-g.

$$I_2 = \frac{\pi}{4} (6^4 - r^4) = 4820 \text{ cm}^4 (115.8 \text{ in.}^4)$$

$$r = 14.8 \text{ cm (5.82 in.)}$$

$$t_2 = 6 - 5.82 = 0.46 \text{ cm (0.18 in.)}$$

$$A_2 = \pi (6^2 - 5.82^2) = 43.2 \text{ cm}^2 (6.684 \text{ in.}^2)$$

$$W_2 = 6.684 \times 0.101 \times 282 = 86.4 \text{ kg (190.38 lb)}$$

$$I_3 = \frac{\pi}{4} (6^4 - r^4) = 2289 \text{ in.}^4 (55.0 \text{ in.}^4)$$

$$r = 15.0 \text{ cm (5.92 in.)}$$

$$t_3 = 0.203 \text{ cm (0.08 in.)}$$

$$A_3 = \pi (6^2 - 5.92^2) = 19.3 \text{ cm}^2 (2.996 \text{ in.}^2)$$

$$W_2 = 2.996 \times 0.101 \times 282 = 38.6 \text{ kg (85.33 lb)}$$

Assuming a minimum wall gauge of 0.06

$$t_4 = 0.06$$

$$I_4 = \frac{\pi}{4} (6^4 - 5.94^4) = 1670 \text{ cm}^4 (40.1 \text{ in.}^4)$$

$$A_4 = \pi (6^2 - 5.92^2) = 14.5 \text{ cm}^2 (2.251 \text{ in.}^2)$$

$$W_4 = 2.251 \times 0.101 \times 36 = 3.72 \text{ kg (8.18 lb)}$$

Since the stiffness (except for I_4 , which is larger) is the same as for the previous case, the deflections under orbiting conditions will be nearly the same as before, i.e., slightly less than 2.02 cm (0.797 in.).

Assuming that the joint mechanism weights are not increased significantly by the increase in tube size, the deflection under one-g due to these weights will be unchanged. This deflection is 11.7 cm (4.62 in.) which was not shown separately before.

With the lighter arm section weights, the deflection due to these items will be less. This deflection was not shown separately but was 29.1 cm (11.42 in.). With the new weights it is only 12.0 cm (4.72 in.).

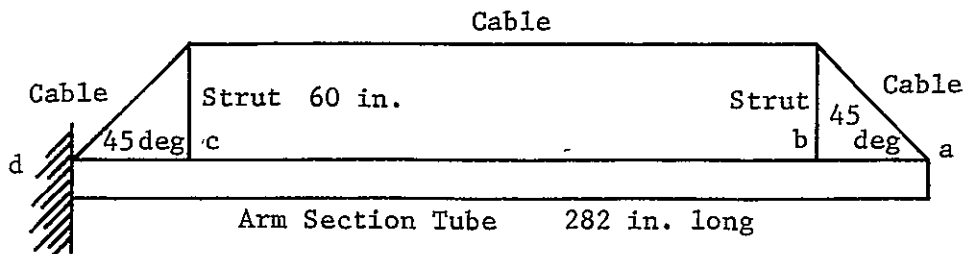
Thus, with 20.3 cm (8.0 in.) arm sections, the total deflection under one-g was $16.04 + 0.797 = 42.7$ cm (16.84 in.) as shown, and with 30.4 cm (12.0 in.) arm is $4.62 + 4.72 + 0.797 = 25.8$ cm (10.14 in.).

The result is a design that has reduced static deflection compared to the 20.3 cm (8 in.) arm in the one-g environment, proper deflection due to design tip loads, reduced weight for joint design considerations, and a reasonable tube size for mounting of the joint mechanisms. Also, the physical appearance is held close to that of the zero-g design.

D. EXTERNAL STIFFENING TECHNIQUE

A possible method of controlling the one-g deflection of a space-design arm is by the temporary addition of rigging cables and compression struts to stiffen the individual sections. This type of support is often used in roof trusses and in pipeline sections across watercourses.

By use of the configuration shown in the sketch each section of the total arm that is primarily loaded in bending may be stiffened with minimum interference at the joints without obscuring the operator's vision. If the sections roll during testing, the sections would have to be stiffened in at least three and probably four planes. Only one plane is shown.



The tube considered is an 8-inch outside diameter aluminum tube with a 0.785 in. wall thickness. Such a tube has a bending moment of inertia of 117.2 in.^4 and a weight per inch of 1.8 lb; $E = 10.7 \cdot 10^6$ psi.

From handbook sources, it can easily be verified that the deflections at points a, b, and c relative to a tangent at d are

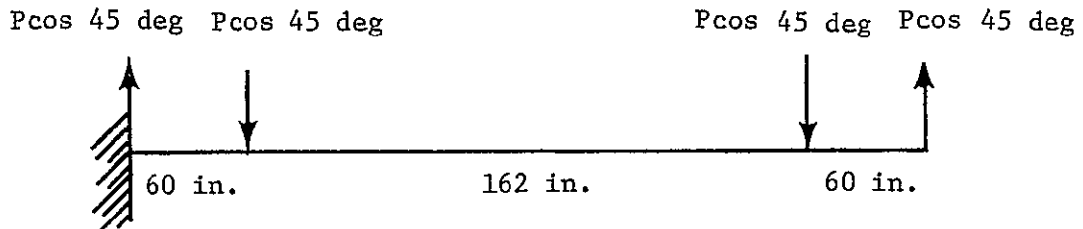
$$\delta_a = 1.133 \text{ in.}$$

$$\delta_b = 0.803 \text{ in.}$$

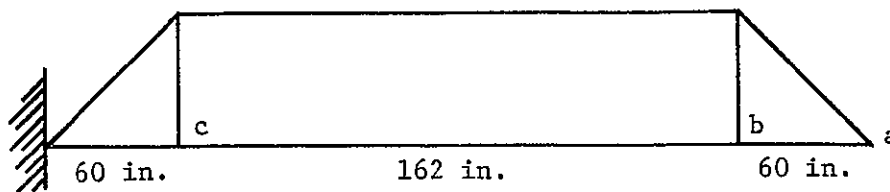
$$\delta_c = 0.083 \text{ in.}$$

under the dead weight of the tube.

The cable can be rigged to any desired tension P, which puts loads and hence moments into the tube as shown below.



The bending moment diagram is $60 P \cos 45 \text{ deg} = 42.43 P$



From the principle of area moments

$$\begin{aligned} \delta_a &= 0.5 \times 60 \times 42.43P \times 242 + 162 \times 47.43P \times 141 + 0.5 \times 60 \\ &\quad \times 42.43P \times 40 \times \frac{1}{EI} \\ &= 308,017P + 969,108P + 50,912P \frac{1}{10.7 \cdot 10^6 \times 117.2} = 0.001059P \end{aligned}$$

$$\begin{aligned}\delta_b &= 0.5 \times 60 \times 42.43P \times 182 + 162 \times 47.43P \times 81 \frac{1}{EI} \\ &= 231,649P + 556,722P \frac{1}{10.7 \cdot 10^6 \times 117.2} = 0.000462P\end{aligned}$$

$$\begin{aligned}\delta_c &= 0.5 \times 60 \times 42.43P \times 20 \frac{1}{EI} \\ &= 25,456 \frac{1}{EI} \\ &= 0.0000203P\end{aligned}$$

The net deflections are then

$$\delta_a = 1.133 - 0.001059P$$

$$\delta_b = 0.803 - 0.000462P$$

$$\delta_c = 0.083 - 0.0000203P$$

It is apparent that a single cable load P cannot be used to reduce all three deflections to zero. However, a cable load in the 1000 to 2000 lb range, which could easily be taken by 0.25-in. aircraft cable (8200 lb), could be used to reduce the bending in the tube to useful limits. A slightly more complicated rigging system could easily be devised to provide more precise bending deflection control.

VII. INVESTIGATION OF OPTIONS FOR SELECTED SIMULATION METHOD (AIRPAD)

The airpad-six degree of freedom simulation method was selected (Chapter V) as the most satisfactory approach for investigating the full size Remote Manipulator System performance. It was recognized that the airpad simulator has a major design problem for large loads in the vertical motion mechanism (air cylinder). A potential practical option of transferring the vertical degree of freedom from the airpad to the Shuttle was proposed. The conditions under which the transfer of the vertical degree of freedom can be made is investigated in this chapter.

Since the airpad simulation method has a significant design problem in only one degree of freedom, it is logical to consider a five-degree-of-freedom simulation. This is especially true considering how readily the five degrees of motion (no vertical) on the airpad simulator can be realized. However, the degradation in simulation validity when going from six degrees of freedom to five would have to be evaluated. This area was not covered in this study. The five-degree airpad simulator does lend itself nicely to the proposed option where the sixth degree is mechanized in the Shuttle mockup. A logical consideration in the evolution of a RMS simulation facility would be to first build a five-degree airpad simulator and later expand the simulator to include the sixth degree.

Considering the above factors, this chapter first covers a five-degree airpad simulator and then the proposed option on the sixth degree of freedom.

A. AIRPAD-FIVE DEGREES OF FREEDOM

A conceptual design of an airpad-five degrees of freedom simulator is shown in Fig. VII-1. This simulator is very similar to the six-degree airpad simulator previously discussed in Chapter IV. However, the simulator structure is significantly less complex because the vertical motion mechanism has been removed. In addition, the concept includes an option of supporting, on separate airpad pedestals, the manipulator arm at the elbow and tip to provide a means of studying the structural bending effects in a planar mode. Only one plane exists in which the manipulator arm can be moved without the elbow translating out of the plane. This plane

VII-2

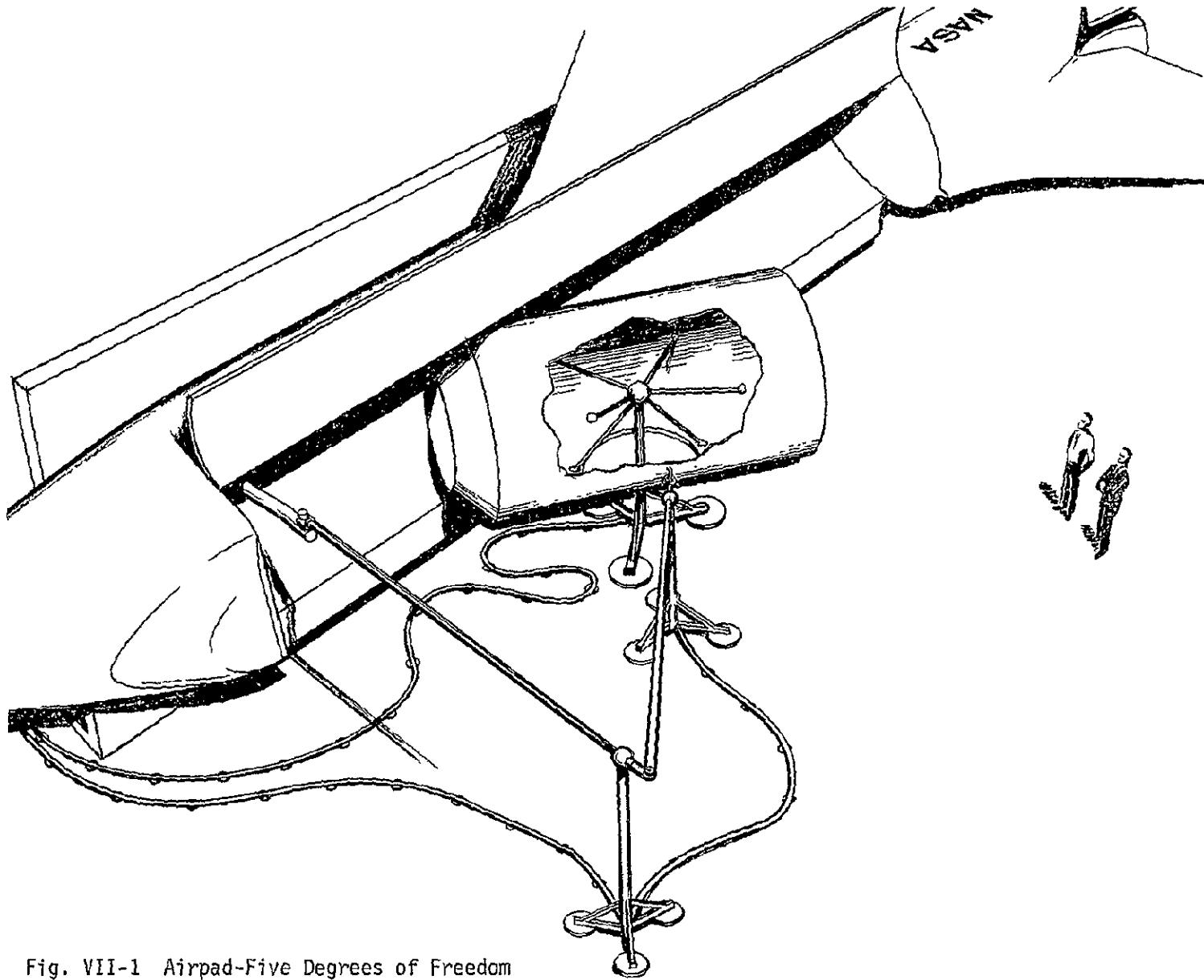


Fig. VII-1 Airpad-Five Degrees of Freedom

passes through the shoulder gimbal axes center of rotation, and the shoulder pitch axis is normal to it. Usage of the airpad pedestals would be restricted to the planar structure bending study. If the airpad pedestals were designed with a telescoping capability, they could be used for all of the RMS control studies.

Removing the vertical degree of freedom from the airpad results in a significant advantage. It allows the target mockup mass to be reduced because the actual target mass can be distributed between the target mockup and the simulator base (Appendix D.2 contains a detailed explanation). This can be done because the same mass (mockup plus simulator) is being moved for all translational motion. Maintaining the actual inertia values for a given physical shape of the target bounds how much the mockup mass can be reduced.

A spherical bearing allowing three degrees of rotational freedom is used in the conceptual simulator design (Fig. VII-1). A considerable advantage resulting from the use of a spherical bearing is that the inertia properties of the target mockup and the simulator base are not coupled. For rotational motion, only the target mockup is moved. Thus, the correct inertias are always being introduced into the dynamics.

B. AIRPAD-FIVE DEGREES AND COUNTERBALANCE-ONE DEGREE

A conceptual design of a proposed airpad-five degrees and counterbalance-one degree simulator is shown in Figure VII-2. This simulator is the natural reaction mode type. It is the same as the five degree airpad simulator discussed previously except for the addition of a vertical degree of freedom. The Shuttle is allowed to move in the vertical direction. In this concept the Shuttle mockup is suspended from a set of vertical guides. Counterweights are used to balance the gravity load. The Shuttle mockup mass plus the counterweight mass is made equal to the target's mass. Air bearings are used in the guides to minimize friction forces.

The functional validity of this simulation concept where the vertical degree of freedom is mechanized in the Shuttle is investigated in Appendix D. The conclusion drawn is that the vertical degree of freedom can be transferred from the target to the Shuttle when the target is sufficiently more massive than the manipulator arm. However, for the smaller targets, this cannot be accomplished without fidelity degradation of the target to Shuttle relative motion. Determination of the errors involved requires a more detailed analysis.

VII-4

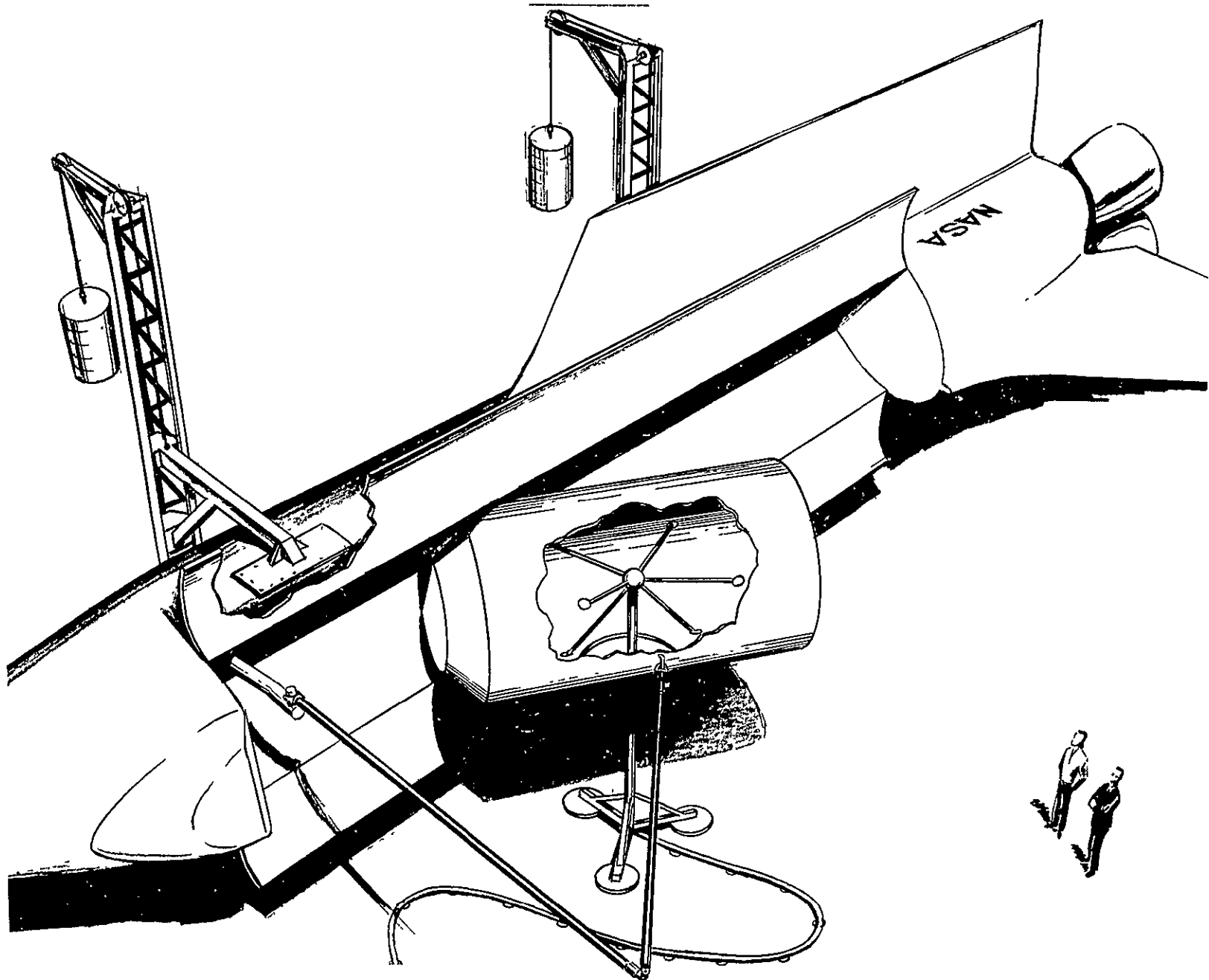


Fig. VII-2 Airpad - Five Degrees and Counterbalance - One Degree

In investigating the above conclusion in light of the design considerations which were the impetus for studying the transfer of the vertical degree of freedom to the Shuttle, an important fact is observed. The airpad vertical motion mechanism design problems were associated with supporting the heavier payloads. However, it is precisely these payloads for which the errors arising from transferring the vertical degree of freedom are minimized. Therefore, a logical conclusion is that an RMS simulation facility should have two classes of airpad simulators. Class I for heavier payloads would be of the type shown in Figure VII-2 where the vertical motion is provided for in the Shuttle mockup. Class II for lighter payloads would be of the type originally proposed (Fig. IV-1) where the vertical motion is provided for by an air cylinder mechanism attached to the airpad base.

VIII. MISSION SIMULATION CAPABILITY OF AIRPAD SIMULATOR

In this chapter, the degree to which the airpad six-degree-of-freedom simulation method is capable of reproducing each of the mission elements described in Chapter II, Section A is considered. The applicability of the Class I and Class II airpad simulators is discussed; Class I being applicable to the heavier payloads and involving vertical motion of the Shuttle mockup; and Class II pertaining to the lighter payloads in which the vertical motion occurs in the payload and Shuttle is fixed.

A. SIMULATOR CAPABILITY BY MISSION ELEMENT

1. Unstowage and Deployment of RMS (Mission Element 1)

Very little error is involved in fixing the Shuttle's translation and rotation when only arm motions are involved. For this reason, the 6 DOF airpad simulation technique can be used, with little or no degradation, to simulate this mission element. Only the Class II simulator is applicable in this case.

2. Berthing Shuttle to Space Station or Other Payloads (Mission Element 2)

It is recalled (Chapter II, Section A), that two alternative functions for the RMS are being considered for this mission element. The one adopted for the purpose of this study involves the manipulator being used strictly as a sensor of the close-in relative position between the Shuttle and the docking target, with only small forces of interaction existing between the bodies. When this is the case, the simulation could be conducted as follows. The Shuttle mockup is fixed in translation and rotation, and the docking target mockup (relatively massless) is mounted on the airpad and given the proper motion relative to the Shuttle. The operator would track the target with the RMS and attach to it. At this time, the RMS is switched to a computer augmented docking mode in which the necessary joint torques would be produced to simulate the relative motion that would occur during actual docking. During the computer-controlled closing stage, the operator would be free to monitor the relative position of the two bodies.

Because the target mockup is envisioned as being relatively massless, only the Class II simulator is applicable to this mission element.

If the second alternative (i.e., where the torque capability of the RMS is used to eliminate or reduce the relative motion) is adopted, then the inertia properties of the target mockup would necessarily be on the order of the Shuttle thereby dictating considerable increases in the work volume of the simulator and the weight that must be supported by the airpad. Because of the larger mass of the target mockup in this case, the Class I simulator would be applicable.

3. Cargo Transfer (Mission Element 3)

During the mission element, the Shuttle is docked to the Space Station, and because of the large combined mass of the two, the translation of the combination can be eliminated with little or no error (provided the mass of the cargo is adjusted in accordance with Eq. [III-1]). It is recalled that the error associated with fixing the translation of the Shuttle is proportional to how small the mass of the manipulator arm is compared to that of the Shuttle/Space Station (See Appendix A). If the residual angular velocity of the Shuttle/Space Station combination is small, the rotational motion of this combination can also be eliminated without seriously degrading the behavior of the system, providing the necessary torque compensation (computer augmentation) is supplied. The degree to which torque compensation is required increases with increasing cargo mass. There again, the Class I simulator will be required for the heavier payloads and the Class II simulator for the smaller payloads.

Thus, the error inherent in using an airpad 6 DOF simulation method will depend on the initial angular velocity of the Shuttle/Space Station and the degree of torque compensation available.

4. Deployment of Payloads (Mission Element 4)

The applicability of the airpad in this case is identical to the previous case except that the error introduced by fixing the Shuttle in translation will be greater than mission element 3 because one is no longer dealing with the Shuttle/Space Station combination; however, as in mission element 3 it can still be expected to be negligible. Assuming there is no residual angular velocity in this case, there will be less error associated with eliminating the rotational motion of the Shuttle. Once again, the Class I simulator can be used for the heavier payloads and the Class II will be required for the smaller payloads.

5. Retrieval of Orbiting Payloads (Mission Element 5)

The applicability of the airpad 6 DOF technique to simulate the mission element is identical to that given for mission element 3. Once again, the errors involved will primarily be due to eliminating the rotation of the Shuttle and will depend on the residual angular velocity of the Shuttle prior to retrieval.

6. Maintenance on Orbiting Vehicles and Payloads - Shuttle Docked (Mission Element 6)

The character of this mission is identical to the cargo transfer mission; hence, the errors involved are of the same type described under mission element 3. The magnitudes of these errors can be expected to be less than those for cargo transfer because of the relatively smaller masses of the replacement modules. Because of the small masses involved, the Class II simulation method must be used.

7. Maintenance on Orbiting Vehicles and Payloads - Shuttle Not Docked (Mission Element 7)

The primary difference between this case and mission 6 is that, in this case, the area to which the replacement modules must be delivered will be moving relative to the Shuttle. The relative motion will be due primarily to the residual linear and angular velocities remaining when the Shuttle's thrusters are shut down. Thus, if the proper initial relative motion can be produced, the error in using the airpad 6 DOF simulation will be the same as in mission element 6. Once again, the Class II simulation technique is required because of the small masses being transferred by the manipulator.

B. SUMMARY

The applicability of the Class I and Class II simulation techniques and the principal sources of error associated with using the 6 DOF airpad simulation method are summarized in Table VIII-1 for each mission element. From this table it can be seen that most of the error arises from eliminating the rotational motion of the Shuttle. As remarked earlier, for those cases where the initial angular momentum of the system is zero, it is expected that most of this error can be eliminated by some form of torque compensation.

Table VIII-1 Airpad Simulator Capability by Mission Element

| DYNAMICAL FEATURES | MISSION ELEMENT | | | | | | |
|---|---------------------------|---------------------|---|---------------------------|---------------------------|---------------------------------|-------------------------------------|
| | 1) UNSTOWAGE & DEPLOYMENT | 2) BERTHING SHUTTLE | 3) CARGO TRANSFER | 4) DEPLOYMENT OF PAYLOADS | 5) RETRIEVAL | 6) MAINTENANCE (SHUTTLE DOCKED) | 7) MAINTENANCE (SHUTTLE NOT DOCKED) |
| Applicability of Class I* or Class II** simulation techniques | Class II only | Class II only | Class I for heavier payloads Class II for lighter payloads | Same as mission element 3 | Same as mission element 3 | Class II only | Class II only |
| Principal sources of error | Little or no error | Little or no error | Error arises from eliminating rotation of Shuttle. The amount will depend on the residual angular velocity of the Shuttle/ space station and the degree of tow torque compensation available. | Same as mission element 3 | Same as mission element 3 | Little or no error | Little or no error |
| *Class I: Airpad simulator for heavier loads (vertical motion on Shuttle mockup) **Class II: Airpad simulator for lighter loads (vertical motion on airpad base) | | | | | | | |

VIII-4

APPENDIX A

DYNAMICAL ANALYSIS

1. Elimination of the Three-Translational-DOF of the Space Shuttle

In this discussion, the Space Shuttle, manipulator upper arm, manipulator forearm, and cargo are modeled as four connected rigid bodies, A, B, C and D (Fig.A-1). Torque producing devices are assumed to act at each of the three connection points.

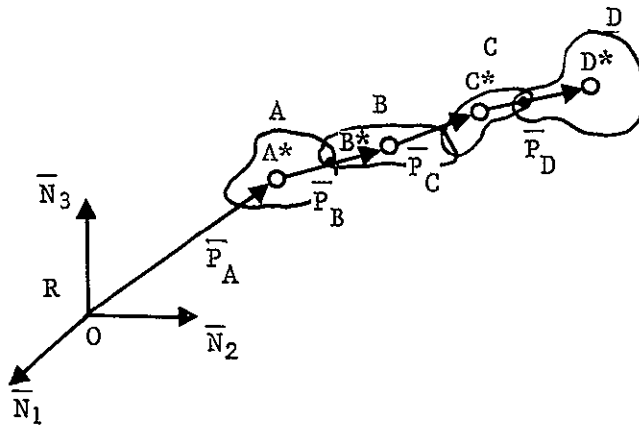


Fig. A-1 Four Connected Rigid Bodies

In Figure A-1, \bar{N}_1 , \bar{N}_2 , and \bar{N}_3 are mutually perpendicular unit vectors fixed in an inertial reference frame R with origin O. The mass centers of A, B, C, and D are designated A*, B*, C*, and D*, respectively. The position of A* relative to O is given by \bar{P}_A ; the position of B* relative to A* is given by \bar{P}_B ; the position of C* relative to B* is given by \bar{P}_C ; and the position of D* relative to C* is given by \bar{P}_D . Finally, the mass of A, B, C, and D are designated M_A , M_B , M_C , and M_D , respectively.

The following scalar quantities prove useful:

$$\begin{aligned}
 P_{Ai} &= \bar{P}_A \cdot \bar{N}_i \\
 P_{Bi} &= \bar{P}_B \cdot \bar{N}_i \quad i = 1, 2, 3 \\
 P_{Ci} &= \bar{P}_C \cdot \bar{N}_i \\
 P_{Di} &= \bar{P}_D \cdot \bar{N}_i
 \end{aligned}
 \tag{A.1.1}$$

The equations of motion of the system described above can be obtained by employing Lagrange's equations

$$\frac{d}{dt} \left(\frac{\partial K}{\partial \dot{q}_r} \right) - \frac{\partial K}{\partial q_r} = Q_r \quad (r = 1, 2, \dots, n)
 \tag{A.1.2}$$

where K is the kinetic energy of the system, q_r is a generalized coordinate, \dot{q}_r is the first time derivative of q_r , and Q_r is the generalized active force associated with q_r , and n is the number of degrees of freedom of the system.

The kinetic energy of the system is

$$\begin{aligned}
 K &= \frac{1}{2} M_A \left(\dot{P}_{A1}^2 + \dot{P}_{A2}^2 + \dot{P}_{A3}^2 \right) + \frac{1}{2} M_B \left[\left(\dot{P}_{A1} + \dot{P}_{B1} \right)^2 + \left(\dot{P}_{A2} + \dot{P}_{B2} \right)^2 \right. \\
 &\quad \left. \left(\dot{P}_{A3} + \dot{P}_{B3} \right)^2 + \frac{1}{2} M_C \left[\left(\dot{P}_{A1} + \dot{P}_{B1} + \dot{P}_{C1} \right)^2 + \left(\dot{P}_{A2} + \dot{P}_{B2} + \dot{P}_{C2} \right)^2 \right. \right. \\
 &\quad \left. \left. + \left(\dot{P}_{A3} + \dot{P}_{B3} + \dot{P}_{C3} \right)^2 \right] \right. \\
 &\quad \left. + \frac{1}{2} M_D \left[\left(\dot{P}_{A1} + \dot{P}_{B1} + \dot{P}_{C1} + \dot{P}_{D1} \right)^2 + \left(\dot{P}_{A2} + \dot{P}_{B2} + \dot{P}_{C2} + \dot{P}_{D2} \right)^2 \right. \right. \\
 &\quad \left. \left. + \left(\dot{P}_{A3} + \dot{P}_{B3} + \dot{P}_{C3} + \dot{P}_{D3} \right)^2 \right] + K_{ROT}
 \end{aligned}
 \tag{A.1.3}$$

where K_{ROT} is the kinetic energy of the system associated with the rotational motion and is, therefore, independent of the P_{Ai} and \dot{P}_{Ai}

($i = 1, 2, 3$). Further, it follows from [A.1.1] that the \dot{P}_{B1} , \dot{P}_{C1} , and \dot{P}_{D1} ($i = 1, 2, 3$) are also independent of the P_{Ai} and \dot{P}_{Ai} .

Now, the only external forces acting on the system are the torques at the connection points and, therefore, there are no generalized active forces associated with the P_{Ai} ($i = 1, 2, 3$). Thus, if one chooses the P_{Ai} for q_i ($i = 1, 2, 3$) it follows from Eq. (A.1.2) that

$$\text{since } \frac{\partial K}{\partial P_{Ai}} = 0$$

$$\frac{\partial K}{\partial P_{Ai}} = C_i \quad (i = 1, 2, 3) \quad [\text{A.1.4}]$$

where the C_i are constants.

The three equations in Eq [A.1.4] can be solved for the \dot{P}_{Ai} and the result substituted into Eq [A.1.3] leaving

$$\begin{aligned} K = \frac{1}{2M_T} \left\{ - \left(C_1^2 + C_2^2 + C_3^2 \right) M_T^2 + M_A \left(M_B + M_C + M_D \right) \left(\dot{\bar{P}}_B \cdot \dot{\bar{P}}_B \right) + \right. \\ \left. \left(M_A + M_B \right) \left(M_C + M_D \right) \left(\dot{\bar{P}}_C \cdot \dot{\bar{P}}_C \right) + M_D \left(M_A + M_B + M_C \right) \left(\dot{\bar{P}}_D \cdot \dot{\bar{P}}_D \right) \right. \\ \left. + 2 M_A \left(M_C + M_D \right) \left(\dot{\bar{P}}_B \cdot \dot{\bar{P}}_C \right) + 2 M_A M_D \dot{\bar{P}}_B \dot{\bar{P}}_D \right. \\ \left. + 2 M_D \left(M_A + M_B \right) \left(\dot{\bar{P}}_C \cdot \dot{\bar{P}}_D \right) \right\} + K_{\text{ROT}} \end{aligned} \quad [\text{A.1.5}]$$

where

$$M_T = M_A + M_B + M_C + M_D \quad [\text{A.1.6}]$$

Finally, where Eq [A.1.5] is substituted into Eq [A.1.2], one is left with N-3 differential equations for the motion of bodies B, C, and D relative to body A.

To determine the kinetic energy of the system when the mass center of A is fixed in inertial space, one merely has to set the P_{Ai} in Eq [A.1.3] equal to zero; this leads to

$$K' = \frac{1}{2} \left[\begin{aligned} & \left(M'_B + M'_C + M'_D \right) \left(\dot{\bar{P}}_B \cdot \dot{\bar{P}}_B \right) + \left(M'_C + M'_D \right) \left(\dot{\bar{P}}_C \cdot \dot{\bar{P}}_C \right) + M'_D \left(\dot{\bar{P}}_D \cdot \dot{\bar{P}}_D \right) \\ & + 2 \left(M'_C + M'_D \right) \left(\dot{\bar{P}}_B \cdot \dot{\bar{P}}_C \right) + 2 M'_D \left(\dot{\bar{P}}_B + \dot{\bar{P}}_D \right) + 2 M'_D \left(\dot{\bar{P}}_C \cdot \dot{\bar{P}}_D \right) \end{aligned} \right] \\ + K_{ROT} \quad [A.1.7]$$

where K' denotes the kinetic energy of the system when A^* is fixed in R, and M'_B , M'_C , M'_D denote the masses of bodies B, C, and D to distinguish them from M_B , M_C , and M_D in Eq [A.1.5]. Thus, when Eq [A.1.6] is substituted into Eq [A.1.2] one obtains the N-3 differential equations for the motion of bodies B, C, and D relative to A when A^* is fixed in R.

Now, it follows from Eq [A.1.2] that when

$$K' = K + \text{Const}, \quad [A.1.8]$$

the equations for the motion of B, C, and D relative to A (and, therefore, the motion itself) will be identical. Comparison of Eq [A.1.5] and Eq [A.1.6] reveals that this will be the case when

$$M'_B + M'_C + M'_D = \frac{M_A (M_B + M_C + M_D)}{M_T} \quad [A.1.9]$$

$$M'_C + M'_D = \frac{(M_A + M_B) (M_C + M_D)}{M_T} \quad [A.1.10]$$

$$M'_D = \frac{M_D (M_A + M_B + M_C)}{M_T} \quad [A.1.11]$$

$$M'_C + M'_D = \frac{M_A (M_C + M_D)}{M_T} \quad [A.1.12]$$

$$M'_D = \frac{M_A M_D}{M_T} \quad [A.1.13]$$

$$M'_D = \frac{M_D (M_A + M_B)}{M_T} \quad [A.1.14]$$

It is apparent from Eq [A.1.9] and [A.1.14] that single values for M'_B , M'_C and M'_D cannot be chosen so as to satisfy [A.1.8]. However, if one assumes that $M_B = M_C = 0$, Eq [A.1.9] - [A.1.14] reduce to

$$M'_D = \frac{M_A M_D}{M_A + M_B} \quad [A.1.15]$$

where, it is recalled, M'_D denotes the mass of body D when body A is restrained from translation and M_A and M_D are the masses of body A and B, respectively, when A is free to translate.

Thus, if one assumes that body A represents the Space Shuttle, bodies B and C represent the two segments of the manipulator arm, and body D represents a payload, and if it is further assumed that the motion of the manipulator arm does not appreciably influence the motion of the system*, then it is possible to restrain the translation of the Shuttle and maintain the integrity of the manipulator.payload to Shuttle relative motion by adjusting the mass of the cargo in accordance with [A.1.15].

It is recalled that in the foregoing analysis, it was assumed that the only external forces acting on the system were the torques at the connection points (arm joints). When the manipulator is used in a docking maneuver or for payload retrieval, this is not the case. During such maneuvers, impact forces will occur between body C and body D (Fig. A-1) and these forces will, in general, result in generalized active forces associated with the translation coordinates of the Shuttle. If it is assumed (as is generally the case with impact problems) that the impact results

*See Section 2. for an argument to neglect the influence of manipulator motion on the systems motion.

in an instantaneous change in the velocities of the colliding bodies but no change in their positions, we can conclude that the impact forces are not functions of the positions of the bodies (i.e., they will depend only on the time) which, in turn, means that the generalized active forces associated with the translation of the Shuttle depend only on the time. Thus, the only difference in the formulation of the equations of motion for the collision problem and the foregoing problem (where the payload is attached to the manipulator arm) is in Eq [A.1.4]. The difference is found in the C_i terms. For the collision problem, the C_i will be functions of time, whereas before the C_i were constants. However, as differentiation with respect to time does not occur in Eq [A.1.2], the time-dependent C_i terms will drop out during formulation of the equations of motion just as the constant C_i did in the previous case. Thus, the foregoing conclusions pertaining to fixing the translation of the Shuttle apply equally well to the collision problem.

2. Elimination of the Three Rotational DOF of the Space Shuttle

The generalized approach followed in Section A.1 is considerably more involved when applied to the rotational motion. In lieu of the general case, a simplified planar analysis is presented to arrive at an estimate of the error inherent in fixing the rotational motion of the Shuttle. In so doing, a conservative estimate of the influence of manipulator motion on the system's motion is obtained.

The system to be studied consists of two rigid bodies A and B, the mass centers of which are connected by a massless arm of length L (Fig. A-2). Mutually perpendicular unit vectors \bar{N}_1 , \bar{N}_2 , and \bar{N}_3 are fixed in an inertial reference frame R with an origin O . The mass center of A is located relative to O by the position vector \bar{P} , where

$$\bar{P} = x\bar{N}_1 + y\bar{N}_2 \quad [A.2.1]$$

The orientation of body A in R is given by the angle ϕ and the orientation of body B relative to A is given by the angle θ (i.e., the arm is assumed fixed in B). The masses of A and B are M_A and M_B , respectively. The moments of inertia of A and B about their mass centers in the \bar{N}_3 direction are I_A and I_B respectively, and these are assumed to be principal moments of inertia. A torque of magnitude T is assumed to act at the mass center of A.

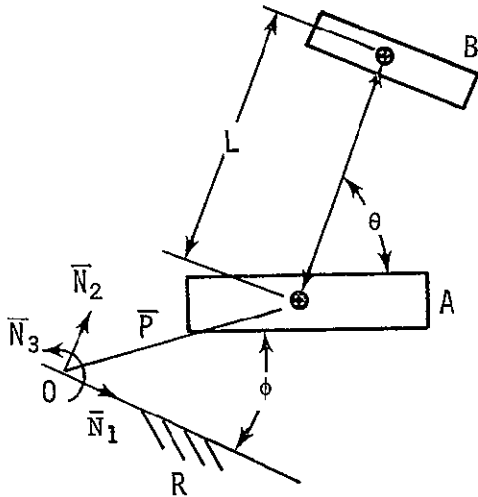


Fig. A-2 Two Connected Rigid Bodies

Using the Lagrangian approach (See Eq [A.1.2].), one obtains the following equations for x , y , ϕ , and θ :

$$\ddot{\theta} = \alpha \Gamma \tag{A.2.2}$$

$$\Delta\phi = -\beta\Delta\theta \tag{A.2.3}$$

$$x = -\frac{M_B}{M_A + M_B} L \cos (\theta + \phi) \tag{A.2.4}$$

$$y = -\frac{M_B}{M_A + M_B} L \sin (\theta + \phi) \tag{A.2.5}$$

where

$$\alpha = \frac{I_A + I_B + \frac{M_A M_B}{M_A + M_B} L^2}{I_A \left(I_B + \frac{M_A M_B}{M_A + M_B} L^2 \right)} \tag{A.2.6}$$

$$\beta = \frac{I_B + \frac{M_A M_B}{M_A + M_B} L^2}{I_A + I_B + \frac{M_A M_B}{M_A + M_B} L^2} \quad [A.2.7]$$

and where it has been assumed that $\dot{x}(0) = \dot{y}(0) = \dot{\phi}(0) = 0$.

From Eq [A.2.3] to [A.2.5], it is possible to estimate the influence of the manipulator mass and inertia on the motion of the system. Using the weight estimates in Table X-3 of MSC 05218, a conservative estimate is obtained by assuming the entire mass of the manipulator arm, 550.5 kg (1212 lb), is concentrated at the end of a 15.25 m (50 ft) arm. The moment of inertia of this mass is determined by assuming the arm segments are homogeneous cylinders which results in a value of 1395 kg-m² (1026 slug-ft²). The mass of the Shuttle is assumed to be 145,000 kg (10⁴ slugs) and its moment of inertia is taken to be 3.1 × 10⁶ kg-m² (2.3 × 10⁶ slug-ft²) (the minimum moment of inertia, for a conservative estimate). Thus in Eq [A.2.3] to [A.2.7] one has

$$M_A = 1.95 \times 10^5 \text{ kg (} 10^4 \text{ slug)}$$

$$I_A = 3.1 \times 10^6 \text{ kg-m}^2 \text{ (} 2.3 \times 10^6 \text{ slug-ft}^2)$$

$$M_B = 550 \text{ kg-m}^2 \text{ (} 37.8 \text{ slugs)} \quad [A.2.8]$$

$$I_B = 1395 \text{ kg-m}^2 \text{ (} 1026 \text{ slug-ft}^2)$$

$$L = 15.25 \text{ m (} 50 \text{ ft)}$$

Substitution of the values in Eq [A.2.8] in [A.2.3] to [A.2.7] leaves

$$\Delta\phi = -0.039\Delta\theta \text{ (rad)}$$

$$x = -0.189 \text{ Cos } (\theta + \phi) \text{ (ft)} \quad [A.2.9]$$

$$y = -0.189 \text{ Sin } (\theta + \phi) \text{ (ft)}$$

Differentiating Eq [A.2.9] with respect to time

$$\dot{\phi} = -0.039 \dot{\theta} \text{ (rad/sec)}$$

$$\dot{x} = +0.182 \dot{\theta} \sin(\theta + \phi) \text{ (ft/sec)} \quad [\text{A.2.10}]$$

$$\dot{y} = -0.182 \dot{\theta} \cos(\theta + \phi) \text{ (ft/sec)}$$

Now, assuming the maximum arm travel is $\theta_{\max} = \pi$ rad, and the maximum arm rate is $\dot{\theta}_{\max} = 0.03$ rad/sec (See Table X-2 of MSC 05218.) the following maximum motions are obtained from Eq [A.2.9] and [A.2.10].

$$\Delta\phi_{\max} = 0.12 \text{ rad (6.3 deg)}$$

$$\dot{\phi}_{\max} = 0.001 \text{ rad/sec (0.057 deg/sec)} \quad [\text{A.2.11}]$$

$$x_{\max} = y_{\max} = 0.055 \text{ m (0.182 ft)}$$

$$\dot{x}_{\max} = \dot{y}_{\max} = 0.0016 \text{ m/sec (0.0055 ft/sec)}.$$

During actual operation, the motion induced by the arms on the Shuttle will always be less than the values given in Eq [A.2.11]. For this reason, it is felt that the Shuttle motion induced by arm motions is negligible and hence the inertia properties of the manipulator arm can be neglected.

In light of the foregoing conclusion and the results of Section A.1, it is seen that it is possible to eliminate the three translational DOF of the Shuttle and maintain the integrity of manipulator/payload to Shuttle relative motion by using an adjusted mass for the payload. (See Eq [A.1.15.] At this point, it is logical to ask if it is possible to eliminate the three rotational DOF of the Shuttle by adjusting the moments of inertia of the cargo. The general approach used in Section A.1 becomes too involved to apply to the rotational motion at this time; however, one can determine the amount of error introduced when the Shuttle is fixed, rotationally, without any adjustment of the inertia properties.

In estimating the aforementioned error, it is assumed that the manipulator arm is capable of performing the task of interest while the Shuttle is fixed.* What this means, is that the operator will exert sufficient torques on the controller to induce a desirable manipulator/payload to Shuttle relative motion. This relative motion will be the same whether or not the Shuttle is fixed. The difference between the fixed Shuttle and free Shuttle cases lies in the forces the operator must exert on the controller. For this reason, the error associated with eliminating the Shuttle's rotational motion is assumed to be the percentage difference in the torque required to perform a particular task when the Shuttle is fixed and when it is free to rotate. In other words,

$$e = \text{percentage error} = \frac{T_f - T}{T} \times 100 \quad [\text{A.2.12}]$$

where T_f denotes the torque required to perform a particular task when the Shuttle is restrained from rotating while T denotes the torque to perform the same task when the Shuttle is free. From Eq [A.2.2] one has

$$e = \frac{\frac{\ddot{\theta}}{\alpha_f} - \frac{\ddot{\theta}}{\alpha}}{\frac{\ddot{\theta}}{\alpha}} \times 100 = \frac{\alpha - \alpha_f}{\alpha_f} \times 100 \quad [\text{A.2.13}]$$

where α_f is obtained from Eq [A.2.6] by assuming I_A and M_A are infinite, or

$$\alpha_f = \frac{1}{I_B + M_B L^2} \quad [\text{A.2.14}]$$

Substitution from Eq [A.2.6] and [A.2.14] into Eq [A.2.13] leaves

*Based on a guideline of the preliminary design, the joint torques were designed for a Shuttle fixed in space; hence the increased "Shuttle fixed" torque capability can be assumed.

$$e = \left[\frac{\left(I_A + I_B + \frac{M_A M_B}{M_A + M_B} L^2 \right) \left(I_B + M_B L^2 \right)}{\left(I_B + \frac{M_A M_B}{M_A + M_B} L^2 \right) I_A} - 1 \right] \times 100 \quad [A.2.15]$$

The values of e for some typical payloads are shown in Table A-1 (The values for I_A , M_A and L are taken from Eq [A.2.8].)

Table A-1 The Increase in Torque Caused by Restraining the Rotational Motion of the Shuttle

| PAYLOAD DESCRIPTION (from Table III-2 of MSC 05218) | e (Eq [A.2.15])* |
|--|------------------|
| Max Orbiter Payload $M_B = 29,400 \text{ kg } (2 \times 10^3 \text{ slugs})$ $I_B = 8.7 \times 10^4 \text{ kg-m}^2 (6.4 \times 10^4 \text{ slug-ft}^2)$ | 240% |
| Space Station Module $M_B = 9050 \text{ kg } (6.2 \times 10^2 \text{ slugs})$ $I_B = 2.3 \times 10^5 \text{ kg-m}^2 (1.7 \times 10^5 \text{ slug-ft}^2)$ | 80% |
| 5000-lb Satellite $M_B = 2270 \text{ kg } (1.55 \times 10^2 \text{ slug})$ $I_B = 9.2 \times 10^3 \text{ kg-m}^2 (6.8 \times 10^3 \text{ slug-ft}^2)$ | 19% |
| Unloaded Arms $M_B = 550 \text{ kg } (37.8 \text{ slugs})$ $I_B = 1395 \text{ kg-m}^2 (1026 \text{ slug-ft}^2)$ | 4% |
| *Based on a guideline of the preliminary design, the joint torques were designed for a fixed Shuttle; hence it is assumed the manipulator is capable of the indicated torque increase. | |

It can be seen from the values in Table A-1 that the increase in the torque requirement brought about by fixing the Shuttle in rotation becomes considerable for the larger payloads. Once again, it is noted that the values in Table A-1 are conservative estimates, and the actual increase in torque can be expected to be somewhat less. Nevertheless, it is apparent that some form of compensation is necessary if the Shuttle's rotation is to be eliminated and the torque requirement is to stay the same. Now, the adjustment in payload mass given by Eq [A.1.15] will aid in decreasing the value of e , and it may be possible to eliminate the torque increase entirely by adjusting the moments of inertia of the payload. The possibility of eliminating e by adjustment in the inertia properties of the payload necessitates a more detailed analytical investigation than is presented here. In the event that the necessary compensation cannot be obtained by adjustment in payload inertia properties, one can always appeal to a computer augmented simulation in which the proper torque compensation is computed by monitoring the motion of the manipulator, and the necessary signals are relayed to the control mechanism thereby giving the operator the proper "feel". It is noted that if force feedback is not to be employed, no compensation is necessary assuming the manipulator is capable of the increased torque requirement.

3. Conclusions

It was shown in Section A.2 that the inertia properties of the manipulator arm have a negligible influence on the system's motion. For this reason (See Section A.1.), it is possible to eliminate the three translational DOF of the Shuttle (during a simulation) by choosing the mass of the payload property. (See Eq [A.1.15].)

It is possible to eliminate the rotational motion of the Shuttle (during a simulation) without any torque compensation for small payloads. (What constitutes a "small" payload will depend on a more detailed analysis.) However, for the larger payloads, some form of torque compensation is necessary if a force feedback type of control is employed. The necessary compensation might be obtained by proper adjustment in payload inertia properties (Whether or not this is possible requires a more detailed investigation.) or by computer augmentation or both. If force feedback is not used, the Shuttle's rotational motion can be eliminated without torque compensation in the master, if one assumes the slave is capable of the increased torque requirement.

APPENDIX B

OPTICAL ROTATION OF RMS OPERATOR'S FIELD OF VIEW

Orientation of the Shuttle on its side as well as the requirement to either rotate the operator on his side also or to rotate his field of view through 90 deg (for direct as opposed to TV viewing of RMS operations) was discussed in Chapter III, Section B. The four methods of rotating the field of view (FOV) which were briefly investigated include the following:

- 1) Dove or Pechan prism;
- 2) Planar mirror system;
- 3) Afocal lens and planar mirror system;
- 4) Aspherical mirror system.

Upon initial examination, these methods appeared to be most feasible methods for rotating the FOV. These should be further analyzed and other techniques investigated. All four methods of rotating the field of view have the following limitations:

- 1) One window - The Shuttle RMS operator as per NASA Drawing No. SAY 44101672 is provided with three rearward facing windows. It is quite likely that small viewing ports will be added on the side and top of the crew compartment for RMS operations. Rotating the field of view can be done only one window at a time and displaces the operator through 90 deg in the yaw axis in addition to the desired 90 deg roll. Therefore, it would be very difficult to maintain the same window relationships when more than one window's FOV is rotated;
- 2) One man operation - The RMS operations are presently designed to use the Shuttle pilot at a rearward facing window. If one wanted to rotate this field of view, the pilot and RMS operator would have to be positioned either in tandem or facing each other and not side by side as they would be nominally (because of the yaw axis rotation requirement just mentioned);
- 3) Small field of view - As discussed below, each of the four methods investigated gives a smaller field of view than that shown in MSC Drawing No. SAY 44101672.

(The RMS operator's field of view will be 68 deg upward, 20 deg downward, 26 deg left and 26 deg right relative to the line-of-sight parallel to the X-axis of the Shuttle.)

1. Dove or Pechan Prism

Two refractive methods of image rotation are demonstrated in the Dove and Pechan Prisms (Fig. B-1). Both methods are useful in a collimated or near collimated system, but neither will accept a field angle larger than about 20 deg.

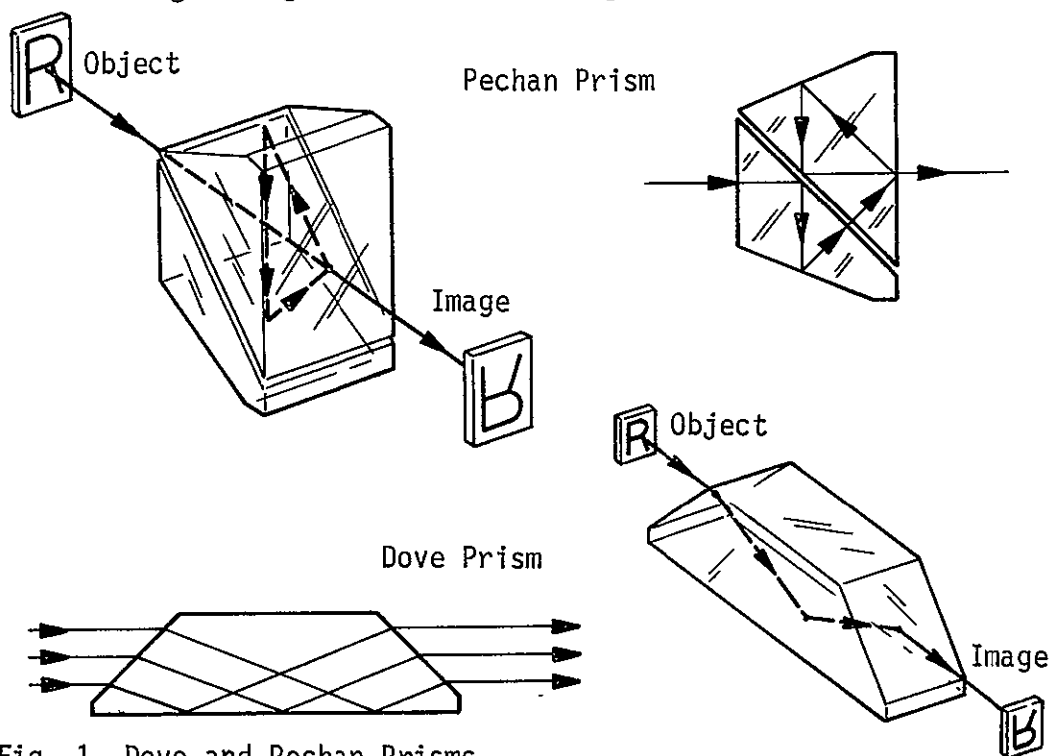


Fig. 1 Dove and Pechan Prisms

2. Planar Mirror System

Based upon MSC Drawing No. SAY 44101672, a mirror system that would rotate the 26 deg/26 deg horizontal, 68 deg/20 deg vertical field was examined. It was determined that the mirror system required was infinitely large. (A 90 deg cone parallel to the X-axis is the theoretical limit making a 68 deg/20 deg vertical FOV impossible.) Therefore, a practical limit was determined to be 25 deg/20 deg vertical and a 26 deg/17 deg horizontal field of view, which requires the following approximate dimensions (Fig. B-2):

- one 4.0 m (13 ft) by 3.8 m (12.5 ft) mirror
- one 1.5 m (5 ft) by 2 m (6.5 ft) mirror;
- a 4.0 m (13 ft) optical path length.

(A 35 deg/0 deg vertical field of view would require mirrors slightly smaller.)

Let us define "viewing plane" as that plane normal to the optical axis and positioned just in front of the mirror closest to the cargo bay. If the viewing plane is at the cargo bay's forward bulkhead (where the RMS operator's window is nominally located), then the operator will perceive the manipulator arms as if he were 4.0 m (13 ft) back from a large window. In other words, the arm would appear 4.0 m further away than nominally. If the viewing plane is positioned 4.0 m (13 ft) into the cargo bay, the operator will have a correct perspective although it will be limited to 45 deg and there will be a 4.0 m (13 ft) foot long protrusion into the front of the cargo bay, which may untealistically interfere with the manipulator arms and/or cargo mockups in that area. (This 4.0 m (13 ft) protrusion would include the mirror system and the crew compartment for the operator.)

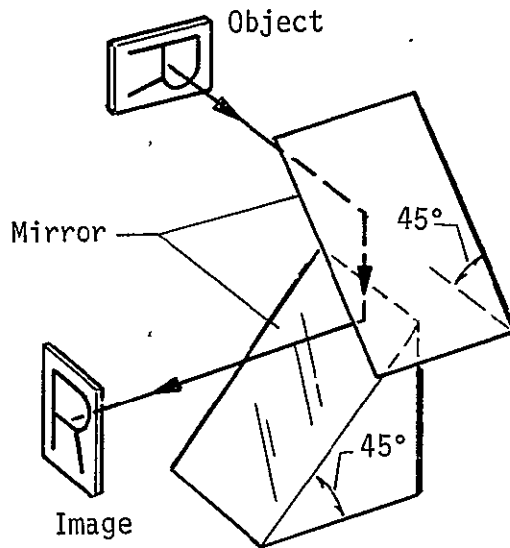


Fig. 2 Planar Mirror System

A primary design consideration is the smoothness of the large mirrors. The surface of the mirror as well as the image will be in focus to the operator. If the surface is wavy, then the image will appear to be wavy also.

3. Afocal Lens and Planar Mirror System

Another method investigated was an afocal lens system similar to a large aperture, unit magnification telescope. Using two small mirrors at 45 deg angles, the reduced internal field is rotated through the required angle. (The lens system rotates the image through 180 deg and, therefore, requires a different mirror arrangement than the previous method.)

The system creates a planar exit pupil the same size as the objective lens with no apparent additional optical path (increased depth) and no magnification. The eye must be within the exit pupil to receive an image (Fig. B-3). An object at a given distance requires the same focus accommodation by the human eye whether seen through the lens system or directly i.e., there is no apparent increase in optical path, no magnification, and no depth of focus problems.

To achieve a large aperture and a short focal length, it is necessary to use a Fresnel lens. After consulting with the major manufacturers of Fresnel lenses, it was determined that the fastest Fresnel lens with good optical properties had an f number of at least 1.0 (although f numbers of 0.5 had been manufactured) and the largest diameter was 178 cm (70 in.), although most manufacturers' limit was less than 51 cm (20 in.). Therefore, using a 178 cm (70 in.) diameter lens with a 178 cm (70 in) focal length, it was determined that the maximum field of view was 24 deg with an 20.3 cm (8 in.) exit pupil (26 deg with a 10 cm exit pupil). The mirrors required are 38 cm (15 in.) and 56 cm (22 in.) and 56 cm (22 in.). Twenty-four degrees is only about ± 3.05 m (± 10 ft) about the X-axis at a 15 m (50 ft) distance. If desired, it appears possible to position this 24 deg cone such that it is not parallel to the X-axis while still keeping the RMS operator vertical.

4. Aspherical Mirror System

The possibility of using two image forming mirrors in a 45 deg off axis configuration was also considered as a solution to both the apparent optical path and image rotation problems. Even if the mirror system could be designed through the use of computer design programs, and if an existing optical industry would accept the task of fabricating the large aspheric mirrors, aberrations would be severe and image quality would be very poor. This is possible in theory but appears impractical to implement.

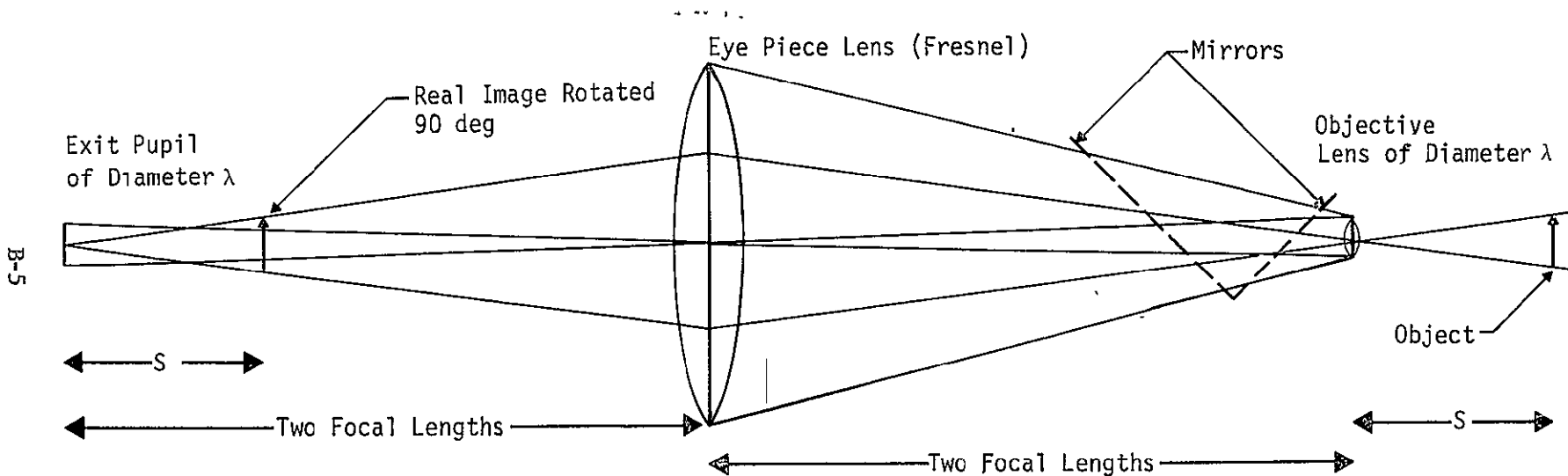


Fig. B-3 Afocal Lens and Planar Mirror Systems

APPENDIX C

CENTER OF GRAVITY LOCATION FOR SIX-DEGREE-OF-FREEDOM AIRPAD
SIMULATOR

In examining the six-degree-of-freedom airpad simulator design shown in Fig. IV-1, the conditions on the structure that must be moved for each motion can readily be determined. These conditions are summarized in Table C-1, and their effects are discussed below.

Table C-1 Simulator Structure Being Moved

| STRUCTURE BEING MOVED | TARGET MOCKUP | ROLL GIMBAL | PITCH GIMBAL | AIR CYLINDER | SUPPORT STRUCTURE WITH AIR PADS |
|-----------------------|---------------|-------------|--------------|--------------|---------------------------------|
| ROLL | X | | | | |
| PITCH | X | X | | | |
| YAW | X | X | X | X | X |
| VERTICAL | X | X | X | | |
| LATERAL | X | X | X | X | X |
| LONGITUDINAL | X | X | X | X | X |

1. Roll Couples

Only the roll inertia of the mockup is being moved. The roll gimbal axis must pass through the cg of the target mockup so the roll gimbal load is balanced. Obviously then, the cg of the target mockup must be located at the cg of the actual target.

2. Pitch Couples

For pitch motion, the inertia being moved is the combination of the target mockup pitch inertia and the roll gimbal structure. The pitch gimbal axis must pass through the cg of the target mockup so that the pitch gimbal load is balanced, requiring balancing of the roll gimbal structure about the pitch axis.

3. Vertical Forces

For vertical motion, the mass being moved is the combination of the target mockup, roll gimbal, pitch gimbal, and partial air cylinder masses.

It is important to examine the effects on rotation when applying a vertical force to the target mockup. A vertical force through the mockup cg will result in only vertical motion, even if the cg of the combined system being moved does not lie on a vertical axis through the mockup cg. This is true because any moments that might result in a case like this are merely reacted into the airpad structure and do not result in motion.

For a vertical force off the mockup's cg, the inertias to be moved will be correct, but the mass to be moved will be the combination. Thus, the direction of translation of motion would be correct, although the magnitude would be proportional to the combined mass.

4. Lateral and Longitudinal Forces

For these motions the mass being moved is the combination of the target mockup and the total simulator structure.

Horizontal forces through the mockup cg will result in a decoupled translational motion only if the cg of the simulator structure lies along a vertical line through the mockup; otherwise the resultant motion would be a coupling having both translation and rotation. The pitch and roll rotational motion would be correct because both the inertias and the axes of rotation are correct. However, the yaw rotational motion would be incorrect because of a wrong inertia and rotational axes.

The translational motion resulting from a horizontal force would have the correct direction. However, the magnitude would be proportional to the combined mass of the system.

5. Yaw Couple

For yaw motion, the inertia being moved is the combination of the target mockup and the total simulator structure. The yaw rotational axis will pass vertically through the combined cg. Thus, if the cg of the simulator does not lie on a vertical line through the cg of the mockup, the yaw rotational axis will be incorrect.

6. Summary

Location of total simulator structure cg - The cg of total simulator must lie on a vertical line through the cg of mockup.

Location of target mockup cg - Mockup cg must be at intersection of roll and pitch gimbal axis.

Mass Distribution between Target Mockup and Simulator Structure - Since the combined masses to be moved in the horizontal directions is different than that to be moved in the vertical direction, the total mass of the target cannot be divided up between the target mockup and the simulator structure. Therefore, the simulator mass must be made as small as possible as compared to the target mass.

Inertia Distribution between Target Mockup and Simulator Structure - Since the orientation of the target mockup changes with respect to the simulator structure, the required target inertias cannot be divided between the target mockup and the simulator structure. Therefore, the simulator inertias must be made as small as possible as compared to the target inertias.

APPENDIX D

DYNAMICAL ASPECTS OF AIRPAD SIMULATIONS

The purpose of this appendix is to investigate two possibilities for reducing the design problems associated with providing the vertical DOF of a massive cargo supported by an airpad/air bearing arrangement. In Section 1, the feasibility of simply fixing the vertical travel of the cargo and releasing the Shuttle in the vertical direction (with appropriate mass adjustment of the Shuttle) is investigated. In Section 2, a redistribution of the cargo mass is studied.

1. Transfer of the Vertical DOF

In light of the results presented in Appendix A, the Shuttle is assumed fixed in translation and rotation while the cargo is free to move with six DOF. An answer to the following question is desired: Can the integrity of the cargo to Shuttle relative motion, i.e., both the appearance and "feel," be maintained when the cargo is prevented from moving vertically and the Shuttle is now permitted vertical travel? To obtain an answer to this question, an approach similar to that followed in Section A.1 is used. First, the kinetic energy expression for the system, when both the Shuttle and cargo have six DOF, is derived. This expression is then modified by the introduction of two sets of appropriate constraint equations. The resulting two kinetic energy expressions are compared to determine the necessary conditions for transferring the vertical DOF from the cargo to the Shuttle.

The kinetic energy expression when both bodies are free is (See Eq [A.1.3].)

$$\begin{aligned} K = & \frac{1}{2} m_A (\dot{p}_{A1}^2 + \dot{p}_{A2}^2 + \dot{p}_{A3}^2) + \frac{1}{2} m_B \left[(\dot{p}_{A1} + \dot{p}_{B1})^2 + (\dot{p}_{A2} + \dot{p}_{B2})^2 + (\dot{p}_{A3} + \dot{p}_{B3})^2 \right] \\ & + \frac{1}{2} m_C \left[(\dot{p}_{A1} + \dot{p}_{B1} + \dot{p}_{C1})^2 + (\dot{p}_{A2} + \dot{p}_{B2} + \dot{p}_{C2})^2 + (\dot{p}_{A3} + \dot{p}_{B3} + \dot{p}_{C3})^2 \right] \\ & + \frac{1}{2} m_D \left[(\dot{p}_{A1} + \dot{p}_{B1} + \dot{p}_{C1} + \dot{p}_{D1})^2 + (\dot{p}_{A2} + \dot{p}_{B2} + \dot{p}_{C2} + \dot{p}_{D2})^2 \right. \\ & \left. + (\dot{p}_{A3} + \dot{p}_{B3} + \dot{p}_{C3} + \dot{p}_{D3})^2 \right] + K_{ROT} \end{aligned} \quad [D.1.1]$$

Assuming body A (See Figure A-1, Appendix A.) represents the Shuttle and body D, the payload, the constraint that the translation of body A is fixed can be written as

$$\dot{P}_{A1} = \dot{P}_{A2} = \dot{P}_{A3} = 0 \quad [D.1.2]$$

If the vertical motion of D (payload) is restrained along with the horizontal motion of A, the necessary constraint equations are

$$\begin{aligned} \dot{P}_{A3} + \dot{P}_{B3} + \dot{P}_{C3} + \dot{P}_{D3} &= 0 \\ \dot{P}_{A1} = \dot{P}_{A2} &= 0 \end{aligned} \quad [D.1.3]$$

The constraint equations reflecting the restrained rotation of A are the same in both cases and hence need not be included in this analysis.

Substitution from [D.1.2] into [D.1.1] and calling the resulting kinetic energy K_1 , leaves

$$\begin{aligned} K_1 &= \frac{1}{2} m_B \left[\dot{P}_{B1}^2 + \dot{P}_{B2}^2 + \dot{P}_{B3}^2 \right] + \frac{1}{2} m_C \left[\left(\dot{P}_{B1} + \dot{P}_{C1} \right)^2 + \left(\dot{P}_{B2} + \dot{P}_{C2} \right)^2 + \left(\dot{P}_{B3} + \dot{P}_{C3} \right)^2 \right] \\ &+ \frac{1}{2} m_D \left[\left(\dot{P}_{B1} + \dot{P}_{C1} + \dot{P}_{D1} \right)^2 + \left(\dot{P}_{B2} + \dot{P}_{C2} + \dot{P}_{D2} \right)^2 + \left(\dot{P}_{B3} + \dot{P}_{C3} + \dot{P}_{D3} \right)^2 \right] \\ &+ K_{ROT} \end{aligned} \quad [D.1.4]$$

When Eq [D.1.3] are used in [D.1.1], the result is

$$\begin{aligned} K_2 &= \frac{1}{2} m_A \dot{P}_{A3}^2 + \frac{1}{2} m_B \left[\dot{P}_{B1}^2 + \dot{P}_{B2}^2 + \left(\dot{P}_{A3} + \dot{P}_{B3} \right)^2 \right] \\ &+ \frac{1}{2} m_C \left[\left(\dot{P}_{B1} + \dot{P}_{C1} \right)^2 + \left(\dot{P}_{B2} + \dot{P}_{C2} \right)^2 + \left(\dot{P}_{A3} + \dot{P}_{B3} + \dot{P}_{C3} \right)^2 \right] \\ &+ \frac{1}{2} m_D \left[\left(\dot{P}_{B1} + \dot{P}_{C1} + \dot{P}_{D1} \right)^2 + \left(\dot{P}_{B2} + \dot{P}_{C2} + \dot{P}_{D2} \right)^2 \right] + K_{ROT} \end{aligned} \quad [D.1.5]$$

By comparison of Eq [D.1.5] and [D.1.4] and using Eq [D.1.3] for \dot{P}_{A3} , one can write

$$K_2 = K_1 + \frac{1}{2} m_B \left[\left(\dot{P}_{C3} + \dot{P}_{D3} \right)^2 - \dot{P}_{B3}^2 \right] + \frac{1}{2} m_C \left[\dot{P}_{D3}^2 - \left(\dot{P}_{B3} + \dot{P}_{C3} \right)^2 \right] + \frac{\dot{P}_{A3}^2}{2} (m_A - m_D) \quad [D.1.6]$$

Now the condition that the relative motion of D to A be the same in both cases can be written

$$K_2 = K_1 \quad [D.1.7]$$

It follows from Eq [D.1.6] and [D.1.7] that

$$m_A = m_D$$

$$m_B = m_C = 0 \quad [D.1.8]$$

since the terms in brackets and \dot{P}_{A3} in Eq [D.1.6] are not, in general, equal to zero.

Thus, in order to transfer the vertical DOF from the cargo to the Shuttle, the mass of the Shuttle must be set equal to the mass of the cargo, and the masses of the two arm segments must be sufficiently small compared to the cargo mass as to be considered massless.

It is worth noting that $m_B = m_C = 0$ was a necessary condition for eliminating the translational motion of the Shuttle in the first place. (See Section A.1.) Further, it was found in Section A.2 that $m_B = m_C = 0$ is a good approximation to the actual case because of the large mass of the Shuttle. In this case, however, the masses of the arm segments (m_B and m_C) must be small compared to the mass of the cargo.

With regard to an airpad simulation, the foregoing conclusions imply that (since the mass of the manipulator is the same for all payloads), one can transfer the vertical DOF from the payload to the Shuttle when the payload is sufficiently more massive than the manipulator arm. However for the smaller payloads, this cannot be

accomplished without degradation in the cargo to Shuttle relative motion. Once again, determination of the errors involved requires a more detailed analysis.

At first glance, the above conclusion might appear rather bleak to one faced with the design problems of the airpad. It is recalled, however, that the original impetus for transferring the vertical DOF was to overcome the structural problems associated with supporting the heavier payloads. It is precisely these payloads for which the errors arising from transferring the vertical DOF are minimized; therefore the airpad need only provide vertical travel for the lighter payloads thereby relieving some of the structural problems.

2. Redistribution of Cargo Mass

It was found in Section 1 that the vertical DOF can be transferred from the cargo to the Shuttle for the heavier cargos and thus relieve the structural problems associated with providing such travel on the airpad. Assuming this to be the case, there remains the problem of supporting a heavy mass on a spherical bearing to provide rotation. The problem can be alleviated somewhat by transferring some of the cargo mass from the air bearing to the support structure of the airpad. This proposal is investigated in the following paragraphs.

The system to be studied (See Fig. D-1) consists of a body C of mass m_1 , and a mass m_2 both supported by an airpad capable of translating without resistance in the horizontal plane. It is assumed that C is supported on the airpad at its mass center C^* by a frictionless spherical bearing. All of the external forces acting on the system are assumed to be equivalent to a force \bar{F} and a torque \bar{T} acting at C^* . Finally, it is assumed that C^* and m_2 are restrained from any vertical motion.

Because C is supported on a frictionless bearing, the mass m_2 and the airpad structure can only exert a force \bar{F}_2 on C. (See Fig. D-1(b).) If \ddot{a}_1 and \ddot{a}_2 denote the accelerations of body C and mass m_2 , respectively, it follows from Newton's second law that

$$\bar{F} + \bar{F}_2 = m_1 a_1 \quad [D.2.1]$$

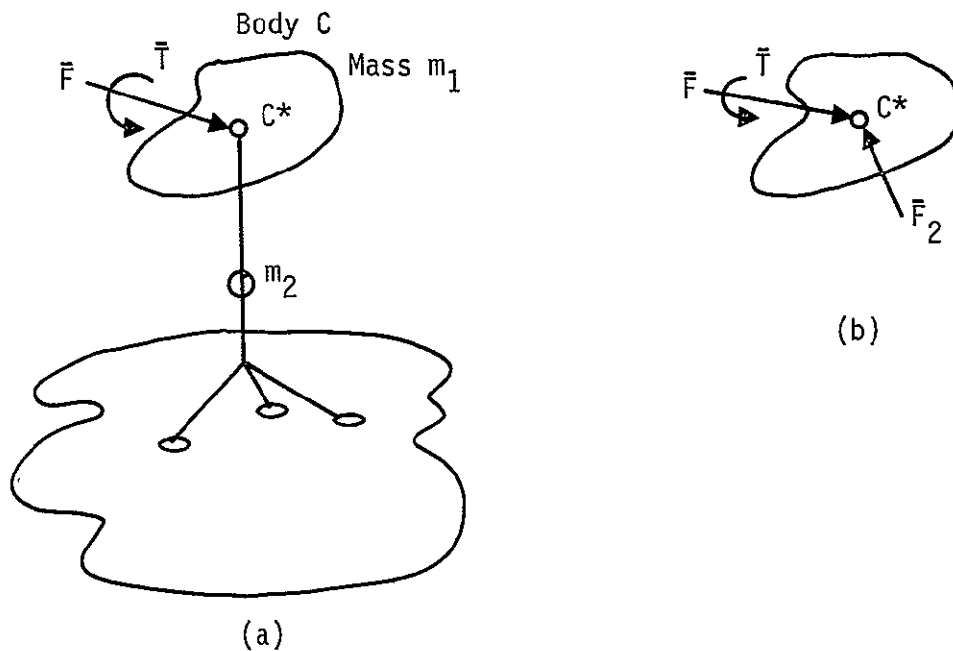


Fig. D-1 Cargo Supported by an Air Bearing

Assuming that the mass of the airpad structure is negligible compared to m_2 , and since there is no friction between the airpad and floor, one can write

$$\bar{F}_2 = -m_2 \ddot{a}_2. \quad [D.2.2]$$

Finally, assuming the airpad support structure is rigid

$$\ddot{a}_2 = \ddot{a}_1. \quad [D.2.3]$$

Combining Eq [D.2.1] and D.1.3]

$$\ddot{a}_1 = \frac{\bar{F}}{m_1 + m_2}. \quad [D.2.4]$$

Thus, if m_C denotes the mass of the cargo, and if m_1 and m_2 are chosen so that Eq [D.2.3]

$$m_1 + m_2 = m_C, \quad [D.2.5]$$

the motion of the system will be the same as if the entire mass of the cargo were supported by the spherical bearing.

The limitation on the amount of mass m_2 that can be transferred to the airpad structure is determined by the inertia properties of the cargo. For example, let $\bar{n}_1, \bar{n}_2, \bar{n}_3$ be mutually perpendicular unit vectors fixed in C and parallel to the principal axes of C for C*, and let

$$\bar{T} \cdot \bar{n}_i = T_i \quad i = 1, 2, 3 \quad [D.2.5]$$

and

$$\overset{R-C}{w} \cdot \bar{n}_i = w_i \quad [D.2.6]$$

where $\overset{R-C}{w}$ denotes the angular velocity of C in an inertial reference frame R. Now the rotational motion of C can be described by Euler's dynamical equations

$$\begin{aligned} I_1 \dot{w}_1 + w_2 w_3 (I_3 - I_2) &= T_1 \\ I_2 \dot{w}_2 + w_3 w_1 (I_1 - I_3) &= T_2 \\ I_3 \dot{w}_3 + w_1 w_2 (I_2 - I_1) &= T_3 \end{aligned} \quad [D.2.7]$$

where I_1, I_2, I_3 are the principal moments of inertia of C for C*.

From Eq [D.2.7] it can be seen that the rotational motion of C will be preserved when mass is transferred to the airpad structure if the principal moments of inertia for the mass center are preserved.

If it is assumed that the cargo is a homogeneous cylinder of mass m_C , radius r , and length ℓ , the principal moments of inertia for the mass center are

$$\begin{aligned} I_1 &= \frac{m_C r^2}{2} \\ I_2 = I_3 &= m_C \left(\frac{r^2}{4} + \frac{\ell^2}{12} \right) \end{aligned} \quad [D.2.8]$$

where it has been assumed that \bar{n}_1 is parallel to the axis of the cylinder [Fig. D-2(a)]. Now, by concentrating masses m_{C1} and m_{C2} at the

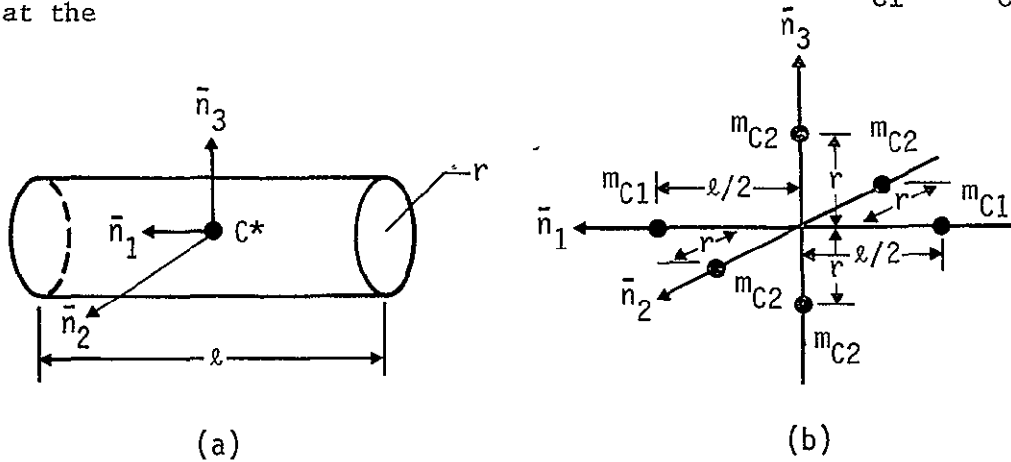


Fig. D-2 Mass Distribution for a Cylindrical Cargo

extremities of the cylinder (Fig. D-2(b), it is possible to reduce the mass of C and preserve the principal moments of inertia. For the mass distribution shown in Fig. D-2(b), the moments of inertia are

$$I_1 = 4m_{C2}r^2$$

$$I_2 = I_3 = \frac{m_{C1}\ell^2}{2} + 2m_{C2}r^2 \quad [D.2.9]$$

Solving Eq [D.2.9] for m_{C1} and m_{C2} , one obtains

$$m_{C1} = \frac{2I_2 - I_1}{2}$$

$$m_{C2} = \frac{I_1}{4r^2}. \quad [D.2.10]$$

The total redistributed mass, m_1 , supported by the spherical bearing is

$$m_1 = 2m_{C1} + 4m_{C2} \quad [D.2.11]$$

To illustrate the foregoing conclusions, assume that the cargo of interest is the maximum orbital payload described in Table A-1, that is

$$m_B = 29.2 \times 10^3 \text{ kg } (2 \times 10^3 \text{ slugs})$$

$$I_1 = 7.75 \times 10^4 \text{ kg-m}^2 \text{ (} 5.7 \times 10^4 \text{ slug-ft}^2\text{)}$$

$$I_2 = I_3 = 8.7 \times 10^4 \text{ kg-m}^2 \text{ (} 6.4 \times 10^4 \text{ slug-ft}^2\text{)} \quad [\text{D.2.12}]$$

Assuming the Shuttle will be fixed during the simulation, the mass of the cargo must be reduced to (See Section A.1.)

$$m_C = \frac{m_B m_A}{m_A + m_B} = 24.5 \times 10^3 \text{ kg } (1.68 \times 10^3 \text{ slugs}) \quad [\text{D.2.13}]$$

where m_A , the mass of the Shuttle, has been taken to be $14.59 \times 10^4 \text{ kg } (10^4 \text{ slugs})$. Now, assuming the length of the cargo is 18.3 m (60 ft) with a 4.6 m (15 ft diameter, or

$$l = 18.3 \text{ m } (60 \text{ ft})$$

$$r = 2.28 \text{ m } (7.5 \text{ ft}) \quad [\text{D.2.14}]$$

it follows from Eq [D.2.10] and [D.2.12] that

$$m_{C1} = 298 \text{ kg } (19.8 \text{ slugs})$$

$$m_{C2} = 3700 \text{ kg } (254 \text{ slugs})$$

So that the total mass on the spherical bearing is (from [D.2.11])

$$m_1 = 15,400 \text{ kg } (1056 \text{ slugs})$$

$$m_2 = m_C - m_1 = 9090 \text{ kg } (624 \text{ slugs})$$

Thus, to simulate the motion of the maximum orbital payload of 29.2×10^3 kg (2×10^3 slugs) a mass of 15.4×10^3 kg (1.056×10^3 slugs) must be supported by the spherical bearing and a mass of 9090 kg (624 slugs) must be attached to the support structure. In other words, one can reduce the mass supported by the spherical bearing by 9090 kg (624 slugs), which represents a decrease of 37% from the adjusted mass of 24,500 kg (1680 slugs). The percentage reduction for smaller payloads will be even greater because the distance from the mass center at which the masses m_{C1} and m_{C2} can be positioned (i.e., l and r) will be same as in the above example, but the moments of inertia I_1 and I_2 in Eq [D.2.10] will be less.

APPENDIX E

STATEMENT OF WORK, TASK IDENTIFICATION

| Chapter | Task No. |
|---|----------|
| II. RMS Mission Requirements | 3.12.1 |
| III. Critical Simulation Requirements | |
| IV. Simulation Methods | 3.12.2 |
| VI. Manipulator Structural Design Alternatives | |
| V. Comparison of Simulation Methods | 3.12.3 |
| VII. Investigation of Options for Selected Simulation Method- Airpad | |
| VIII. Mission Simulation Capability of Airpad Simulation | |